

# Statistical Mechanics of non–reciprocally interacting Ising spins

Author: Adrià Garcés Ortiz\*

*Master en Física dels Sistemes Complexos i Biofísica.*

*Facultat de Física, Universitat de Barcelona, Martí i Franquès 1, 08028 Barcelona, Spain.*†

Advisor: Demian Levis

**Abstract:** Non–reciprocal interactions are present in a large number of out–of–equilibrium systems such as active matter, social, ecological and non–Hermitian quantum systems. They are believed to be responsible for non–equilibrium phase transitions and are, still, an open topic of major interest in recent research. In this work, we present a generalization of the Ising model that includes non–reciprocal interactions among spins and analytically characterize the mean field stationary behaviour of two proposed models that incorporate non–reciprocal interactions. We show how the models exhibit a first order phase transition and how their mean field solutions are no longer spin–inversion symmetric. Furthermore, we also study  $d = 1$  spin chains with nearest neighbours interactions, and derive the evolution equations for the first two moments. Finally, we discuss the dynamical equations for the proposed models. The derived dynamic equations signal the presence of steady currents, e.g. traveling states, in non–reciprocally interacting spin chains.

## I. INTRODUCTION

Newton’s third law, also known as the action–reaction principle, states that the interactions between bodies of a system are symmetric, and thus reciprocal. Systems verifying the action–reaction principle, in the absence of time dependent driving forces, equilibrate into steady (time translational invariant) states which are well described by traditional thermodynamics through the relaxation of their degrees of freedom.

The situation changes when we try to macroscopically describe bodies which are part of a non equilibrium medium, for which the action–reaction principle is not fulfilled. The assumption of reciprocal interactions between particles or agents also breaks down at all scales in a large class of systems such as social systems [1] (pedestrian dynamics, human friendship...), active matter [2–4] (active colloidal mixtures, bio–chemical reactions, bird flocking...) as well as spin–glass (SG) models [5, 6], ecological [7], robotic [8] and non–Hermitian quantum [9] systems.

Non–reciprocal interactions have been, for this reason, of huge interest in recent research and a major and still open topic in non–equilibrium statistical physics [1]. Non–reciprocal interactions usually imply the violation of the detailed balanced condition, preventing the relaxation to equilibrium, and are believed to be responsible for non–equilibrium phase transitions as well as time dependent and traveling states [10, 11]. It has been claimed that they are able to portray self–organizing behaviour such as synchronization, flocking and pattern formation.

Equilibrium problems are well defined and can be studied with conventional, equilibrium, statistical mechanics. However, studying out–of–equilibrium processes

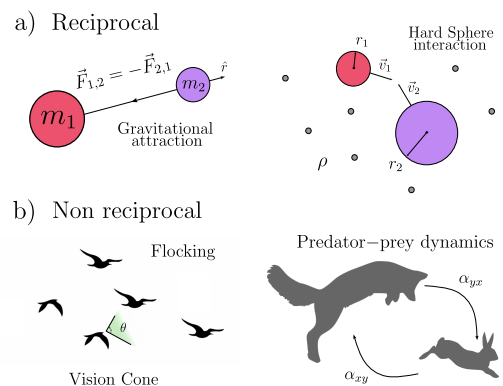


FIG. 1: Examples of reciprocal interactions (a) gravitational attraction between bodies and interaction between hard spheres in a solvent; and non–reciprocal ones (b) vision cones in bird flocking and predator–prey dynamics.

can be challenging, since there is not yet such a general approach. It is common, in this case, to study out–of–equilibrium processes from a dynamic point of view, with stochastic models, for which one can write, in the Markovian case, Master and Fokker–Planck equations.

Throughout this project we attempt to study what happens when non–reciprocal interactions appear due to a state dependence of the coupling between Ising spins, using a simple model. In order to keep the problem as simple as possible, one can first try introducing the possibility of having non–reciprocal interactions in the Ising model, as it is, to date, the canonical model to study spontaneous phase transitions with symmetry breaking. The Ising model’s Hamiltonian reads,

$$\mathcal{H} = - \sum_{i,j} J_{ij} \sigma_i \sigma_j - \sum_{i=1}^N h_0^i \sigma_i, \quad (\text{I.1})$$

where  $\sigma_i = \pm 1, i = 1, \dots, N$  represent the spin variables of the system,  $h_0^i$  accounts for the external field acting

\*Electronic address: [adria.garces@gmail.com](mailto:adria.garces@gmail.com)

†Electronic address: [master.complex.biophys@ub.edu](mailto:master.complex.biophys@ub.edu)

on  $\sigma_i$  and  $J_{ij}$  the coupling matrix. When the coupling is reciprocal,  $J_{ij} = J_{ji}$ , the Ising model's thermodynamics can be derived analytically in some cases and its dynamics is governed by the minimization of energy. When  $J_{ij} \neq J_{ji}$  the definition of a Hamiltonian is ambiguous: the energy of a pair is not univocal,  $J_{ij}\sigma_i\sigma_j \neq J_{ji}\sigma_j\sigma_i$ . Generally speaking, the dynamics are no longer governed by a minimization principle. Due to the lack of an unambiguously defined Hamiltonian, our starting point to understand how non-reciprocal interactions may affect the Ising model's known phase transitions will be the kinetic Ising model. The report is organized as follows: in section Sec. II we review the already known results of the kinetic Ising model, using Glauber dynamics, in the mean field approximation and for  $d = 1$  Ising chains. The results of our work are presented in sections Sec. III and Sec. IV; in section Sec. III we present an extension of the Ising model that includes non-reciprocal interactions and in Sec. IV we discuss non-reciprocal  $d = 1$  spin chains. Section Sec. V concludes.

## II. THE KINETIC ISING MODEL

Stochastic kinetic models have been used to study a great variety of processes. The Ising model's stochastic dynamics in  $d = 1$  was first studied by Glauber [12]. It considers  $N$  spins represented by the stochastic variables  $\sigma_i(t)$  with  $i = 1, \dots, N$ . Since  $\sigma_i(t)$  represent stochastic Ising variables, they are restricted to the values  $\sigma_i(t) = \pm 1$  and can transition randomly between these two. The random transitions take place as we consider the spins to be in contact with a thermal bath at temperature  $T$ .

These transitions occur with a given probability (the transition probability) which depends on the momentary state of neighbouring spins and the temperature of the bath,  $T$ . These transitions can happen in different ways but, in order to simplify the problem, one usually considers transitions at the individual level, and call these transition probabilities spin flip rates. These determine, depending on the neighbouring spin states and the temperature of the bath, the probability that a single spin flips. Since a single spin is flipped with certain probability, the total magnetization of the system is not conserved.

As these transition probabilities only depend on the momentary state of the the neighbouring spins, we can say that the stochastic spin variables  $\sigma_i(t)$  form a continuous time Markovian process. Attributed to this Markovian process, we have a probability function  $p(\boldsymbol{\sigma}; t)$  that measures the probability of finding any of the  $2^N$  possible configurations of the spin variables  $\boldsymbol{\sigma} = (\sigma_1, \dots, \sigma_N)^T$  at time  $t$ . Given the probability that  $\sigma_i$  jumps to the value  $-\sigma_i$ , the spin flip rate  $\omega(\sigma_i)$ , and since these represent a Markovian process,  $p(\boldsymbol{\sigma}; t)$  will obey the Master Equation (ME)

$$\frac{\partial p(\boldsymbol{\sigma}; t)}{\partial t} = \sum_i \omega(\sigma^i) p(\boldsymbol{\sigma}^i; t) - \omega(\sigma_i) p(\boldsymbol{\sigma}; t), \quad (\text{II.1})$$

where now  $\boldsymbol{\sigma} := (\sigma_1, \dots, \sigma_i, \dots, \sigma_N)^T$  so that  $\boldsymbol{\sigma}^i :=$

$(\sigma_1, \dots, -\sigma_i, \dots, \sigma_N)^T$  represents the configuration  $\boldsymbol{\sigma}$  with spin  $i$  flipped, while  $\omega(\sigma_i)$  and  $\omega(\sigma^i)$  represent the spin flip rates of  $\sigma_i$  and  $-\sigma_i$ . Note how the superindex just refers to a change of sign,  $\sigma^i := -\sigma_i$ . The ME represents a balance of probability flux between jumping out of configuration  $\boldsymbol{\sigma}$  by flipping  $\sigma_i$  and jumping into configuration  $\boldsymbol{\sigma}$  by coming from configuration  $\boldsymbol{\sigma}^i$  and flipping  $-\sigma_i$ .

The connection between this stochastic, dynamical, process and the Ising model arises from a proper definition of the spin flip rates. This comes from imposing that the stationary solution of the ME in equation Eq. (II.1) is nothing but the Boltzmann distribution of the Ising model. This is done by demanding that the stationary solutions  $p_s(\boldsymbol{\sigma})$  are time invariant,  $\partial_t p_s(\boldsymbol{\sigma}) = 0$  and are actually Boltzmann distributions,  $p_s(\boldsymbol{\sigma}) := P_{eq}(\boldsymbol{\sigma})$ , such that, the spin flip rates fulfill the detailed balance condition (DB),

$$\omega(\sigma^i) P_{eq}(\boldsymbol{\sigma}^i) = \omega(\sigma_i) P_{eq}(\boldsymbol{\sigma}). \quad (\text{II.2})$$

Note how there is a double implication between the DB condition and Boltzmann distributions. As long as the DB condition holds, we know the probabilities involved in a ME like the one in equation Eq. (II.1), will converge to the equilibrium distribution in the long time limit,  $\lim_{t \rightarrow \infty} p(\boldsymbol{\sigma}; t) = P_{eq}(\boldsymbol{\sigma})$  [13]. As we know, these equilibrium probabilities take the shape

$$P_{eq}(\boldsymbol{\sigma}) = \frac{1}{\mathcal{Z}} e^{-\beta \mathcal{H}(\boldsymbol{\sigma})}, \quad \mathcal{Z} = \sum_{\{\boldsymbol{\sigma}\}} e^{-\beta \mathcal{H}(\boldsymbol{\sigma})} \quad (\text{II.3})$$

where the sum is run over all the possible  $2^N$  configuration of  $\boldsymbol{\sigma}$ ,  $\mathcal{H}(\boldsymbol{\sigma})$  is the Hamiltonian of the Ising model in equation Eq. (I.1) and  $\beta = 1/k_B T$ , where  $T$  is the temperature and  $k_B$  Boltzmann's constant. As a consequence, then, one can define spin flip rates that verify the DB condition the following way [12, 14],

$$\omega(\sigma_i) = \frac{1}{2} [1 - \sigma_i \tanh \beta h_i], \quad (\text{II.4})$$

where  $\beta = 1/k_B T$ , and where

$$h_i = h_0^i + \sum_{j=1}^N J_{ij} \sigma_j, \quad (\text{II.5})$$

is the local field acting on  $\sigma_i$ . Here,  $h_0^i$  accounts for possible external fields acting on  $\sigma_i$ .

The probabilities  $p(\boldsymbol{\sigma}; t)$  solution of the ME in equation Eq. (II.1) provide a full description of the system. However, integrating the ME is generally impossible. Even though we cannot generally integrate these, one can derive simpler equations for both the spin expectation value and correlation function from equation Eq. (II.1), and these two already provide much insight on the large scale behaviour. We define the expectation value of spin  $\sigma_i(t)$  as

$$\langle \sigma_i \rangle(t) := \sum_{\{\boldsymbol{\sigma}\}} \sigma_i p(\boldsymbol{\sigma}; t), \quad (\text{II.6})$$

where, again, the sum is performed over all the possible  $2^N$  configurations of  $\sigma$ , and  $p(\sigma; t)$  is solution to the ME, Eq (II.1). Samewise, we define the correlation function as the expectation value of the product  $\sigma_i \sigma_j$ ,

$$\langle \sigma_i \sigma_j \rangle(t) := \sum_{\{\sigma\}} \sigma_i \sigma_j p(\sigma; t), \quad (\text{II.7})$$

The correlation function in Eq. (II.7) is properly defined since  $\langle \sigma_i(t) \sigma_i(t) \rangle = 1$ , for any  $t$ . Using, then, these two definitions, one can see how, from the ME,  $\langle \sigma_i \rangle(t)$  and  $\langle \sigma_i \sigma_j \rangle(t)$  verify (see Appendix A for derivation),

$$\frac{d\langle \sigma_i \rangle}{dt} = -2\langle \sigma_i \omega(\sigma_i) \rangle \quad (\text{II.8})$$

$$\frac{d\langle \sigma_i \sigma_j \rangle}{dt} = -2\langle \sigma_i \sigma_j [\omega(\sigma_i) + \omega(\sigma_j)] \rangle. \quad (\text{II.9})$$

As we will see, these two equations can be solved easily in some particular cases. We will first consider reciprocally coupled Ising spins for which solutions are known [12, 14], and then try to generalize these for non–reciprocally interacting spins.

### A. Mean Field Ising Model

The mean field (MF) approximation, as we know, consists on substituting spin–spin interactions by a local field acting on each spin, that is, turning  $N$ –body interactions into a single body problem. This can be done with the Ising Hamiltonian in equation Eq. (I.1) but, as we will see, also in the kinetic Ising model. By transforming two body interactions into the coupling of each spin with a local field, we force spins to be uncorrelated, and thus  $\langle \sigma_i \sigma_j \rangle = \langle \sigma_i \rangle \langle \sigma_j \rangle$  for any  $i \neq j$ .

Eventhough the MF approximation can be done for any  $d$ –dimensional lattice provided the coordination number  $z(d)$ , it is equivalent to the fully connected (FC) Ising model, for which every spin interacts with any other spin of the system, hence loosing the notion of spin lattice model and, eventually, the concept of nearest neighbour and geometry. The local field acting on each spin represents, now, a global field.

In the FC Ising model, we have  $J_{ij} = J(1 - \delta_{ij})$  where  $J$  is the coupling constant. The field, now global, acting on  $\sigma_i$  is

$$h_i = h_0^i + J \sum_{j \neq i} \sigma_j, \quad (\text{II.10})$$

so that, defining the magnetization of the system as  $m = (1/N) \sum_j \sigma_j$ , we can then approximate  $h_i$  by setting  $J \sum_{j \neq i} \sigma_j = NJ(1/N) \sum_{j \neq i} \sigma_j \approx NJm$ . Note how the thermodynamic limit  $N \rightarrow \infty$  can be taken by setting  $J = 1/N$  so that the field  $h_i$  is well defined. Considering now no external field acting on  $\sigma_i$ ,  $h_0^i = 0$ , we will have that  $h_i = NJm$ . The spin flip rate of spin  $\sigma_i$  will become

$$\omega(\sigma_i) = \frac{1}{2} [1 - \sigma_i \tanh \beta NJm]. \quad (\text{II.11})$$

As a consequence, the dynamical equation for the expected value of spin  $\sigma_i$ , following equation Eq. (II.8), becomes, using that  $\sigma_i^2(t) = 1$ ,

$$\frac{d\langle \sigma_i \rangle}{dt} = -\langle \sigma_i \rangle + \tanh \beta NJm. \quad (\text{II.12})$$

Dividing this one by  $N$  and summing over all the spins we can find the dynamical equation for the mean magnetization  $m$ , which reads,

$$\frac{dm}{dt} = -m + \tanh \beta NJm. \quad (\text{II.13})$$

Generally, we will say that  $dm/dt = \varphi(m; \beta)$ . The stationary solutions of equation Eq. (II.13),  $dm(t)/dt = 0$ , represent equilibrium magnetization states. We call these self consistent (SC) states, and they verify what is called the self consistent equation  $\varphi(m; \beta) = 0$ . They are equilibrium states since the stationary solutions represent the long time limit behaviour, when the probabilities in the ME converge to the equilibrium distributions. Furthermore, spin flip dynamics do not conserve the order parameter, and thus belong to the universality class of model A [15], so that,

$$\frac{dm}{dt} = -\frac{\partial \mathcal{F}}{\partial m} + \eta(t), \quad (\text{II.14})$$

where  $\eta(t)$  is a Gaussian white noise with zero mean  $\langle \eta(t) \rangle = 0$  and  $\langle \eta(t) \eta(t') \rangle = 2\gamma k_B T \delta(t - t')$ , where  $\delta(t)$  is Dirac's distribution. This is telling us that  $m$  relaxes through the minimization of  $\mathcal{F}$ . Here,  $\mathcal{F}$  represents the MF free energy of the system, since the stationary solutions are just the solutions that minimize  $\mathcal{F}$ . This one can be integrated easily, finding that,

$$\mathcal{F} = \mathcal{F}_0(\beta) - \int \left\{ -m + \tanh \beta NJm \right\} dm, \quad (\text{II.15})$$

which, for small  $m$  reads,

$$\mathcal{F} = \mathcal{F}_0(\beta) - \frac{1}{2}(K-1)m^2 + \frac{1}{12}K^3m^4 + \mathcal{O}(m^6), \quad (\text{II.16})$$

where  $K = \beta NJ$ . The latter is the MF free energy one can find taking the MF approximation in order to compute the equilibrium partition function through the Hamiltonian in Eq. (I.1). We know then, these are the equilibrium solutions of  $m$ , and, when  $J = 1/N$ , the system shows a phase transition at  $K_c = 1$ , with critical exponent  $\beta = 1/2$ , since  $|m| \sim \sqrt{3(K-1)}$ . These results are the well known MF results of the Ising model. All the other critical exponents can be derived from the integrated free energy.

Note how in the high temperature limit,  $\beta \rightarrow 0$ , one can expand the hyperbolic tangent in equation Eq. (II.13) and find that  $dm/dt = -(K_c - K)m - \frac{1}{3}(Km)^3 + \mathcal{O}(m^5)$ . The solutions up to order  $\sim \mathcal{O}(K)$  become  $m \sim e^{-t/\tau}$ , where  $\tau = (K_c - K)^{-1}$ . Here  $\tau$  represents a

characteristic relaxation time which diverges at the critical point  $K = K_c$ . At the critical point, instead, the relaxation happens through a power-law decay, since now  $dm/dt = -K_c^3 m^3/3 + \mathcal{O}(m^5)$ , for which  $m \sim t^{-1/2}$ , with critical exponent  $1/2$ , as expected for the universal class of model A.

### B. Dynamical Behaviour of an Ising Chain

The case of a  $d = 1$  Ising chain of interacting spins was first studied by Glauber [12]. Considering that spins only interact up to nearest neighbours in the chain,  $J_{ij} = J(\delta_{i-1,j} + \delta_{i+1,j})$ , one can compute the partition function of the system and derive the system's thermodynamics. By doing so, it can be seen how there is no phase transition for the Ising chain. These are well known results.

What can also be done is studying the dynamical properties of the Ising chain, in order to understand how it relaxes to equilibrium. The fact that spin interactions are now between first neighbours makes the field  $h_i$  local. The spin flip rates of a single spin  $\sigma_i$  will depend on the local driving field from the neighbouring spins,  $\sigma_{i-1}$  and  $\sigma_{i+1}$ . When this is the case, the spin flip rates become

$$\omega(\sigma_i) = \frac{1}{2} \left[ 1 - \gamma \sigma_i \left( \frac{\sigma_{i-1} + \sigma_{i+1}}{2} \right) \right], \quad \gamma = \tanh 2\beta J. \quad (\text{II.17})$$

These rates come from plugging now the local field  $h_i$  into the Glauber rates in equation Eq. (II.4) and using that  $\tanh \varepsilon x = \varepsilon \tanh x$  when  $\varepsilon = 0, \pm 1$ . The dynamical equations of the expectation value and the correlation function now become

$$\frac{d\langle \sigma_i \rangle}{dt} = -\langle \sigma_i \rangle + \frac{\gamma}{2} [\langle \sigma_{i-1} \rangle + \langle \sigma_{i+1} \rangle] \quad (\text{II.18})$$

$$\begin{aligned} \frac{d\langle \sigma_i \sigma_j \rangle}{dt} = & -2\langle \sigma_i \sigma_j \rangle + \frac{\gamma}{2} [\langle \sigma_{i-1} \sigma_j \rangle + \langle \sigma_{i+1} \sigma_j \rangle \\ & + \langle \sigma_i \sigma_{j-1} \rangle + \langle \sigma_i \sigma_{j+1} \rangle], \end{aligned} \quad (\text{II.19})$$

for  $j \neq i$ . Equation Eq. (II.18) can be integrated by means of defining a generating function in the thermodynamic limit  $N \rightarrow \infty$ . It is convenient labeling a single spin as the one situated at the origin and attributing a negative and a positive integer to each side of the chain, so that now  $i \in \mathbb{Z}$ . By doing so and considering initial condition  $\langle \sigma_i \rangle(0) = \delta_{i,0}$  and  $J > 0$ , the solutions become [12, 14]

$$\langle \sigma_i \rangle(t) = e^{-t} I_i(\gamma t), \quad (\text{II.20})$$

where  $I_i(\gamma t)$  is the modified Bessel function of order  $i$ . This represents the situation in which, initially, the average value of the spin at the origin is 1, while the rest vanish. Equation Eq. (II.20) shows how expectation value of the spin at the origin  $\langle \sigma_0 \rangle$  relaxes steadily to 0, while

the neighbouring ones,  $i \neq 0$ , start growing positively for times  $t \ll |i|/\gamma$  until reaching a maximum as a consequence of the local interactions with  $\sigma_0$ , to later decrease steadily again back to 0 [12]. The long time behaviour of these shows asymptotic decay  $\langle \sigma_i \rangle(t) \approx t^{-1/2} e^{-(1-\gamma)t}$ , again with relaxation time  $\tau = (1-\gamma)^{-1}$ , and power law decay for  $\gamma = 1$ , thus  $T = 0$ . By means of fixing a single spin, one can study the stationary solutions of equation Eq. (II.18). Fixing  $\sigma_0 = 1$ , the steady solution of equation Eq. (II.18) verifies

$$\langle \sigma_i \rangle = \frac{\gamma}{2} [\langle \sigma_{i-1} \rangle + \langle \sigma_{i+1} \rangle], \quad \forall i \neq 0, \quad (\text{II.21})$$

with  $\langle \sigma_0 \rangle = 1$ . The last one is a linear difference equation which can be solved with ansatz  $\langle \sigma_i \rangle = \zeta^{|i|}$ , so that,  $\zeta^2 - 2\gamma^{-1}\zeta + 1 = 0$ . Since  $\zeta$  has to be smaller than one due to the made ansatz, the only possible solution is  $\zeta = \gamma^{-1}(1 - \sqrt{1 - \gamma^2}) < 1$  for any  $\gamma < 1$ . Since by definition we had that  $\gamma = \tanh 2\beta J$ , we have that  $\zeta = \tanh \beta J$ . The same thing can be done for the antiferromagnetic case, for which  $\gamma < 0$  since  $J < 0$ . The general solution for  $i > 0$  can be tackled for any initial configuration of spins as a linear combination of the particular solution in equation Eq. (II.20),

$$\langle \sigma_i \rangle(t) = \zeta^i + e^{-t} \sum_{m=-\infty}^{\infty} \langle \sigma_m \rangle(0) I_{i-m}(\gamma t), \quad (\text{II.22})$$

to which we added the stationary solution, so it becomes the solution in the long time limit. The same approach can be taken in order to solve the equations governing the dynamics of the correlation function. If one considers the system to be translationally invariant, so that the correlation function can only depend on the relative distance between neighbouring spins, one can define  $\mathcal{C}_k(t) = \langle \sigma_i \sigma_{i+k} \rangle$ , for any  $k \neq i$  under the condition  $\mathcal{C}_0(t) := \langle \sigma_i^2(t) \rangle = 1$  for any  $t$ . Equation Eq. (II.19) thus reads,

$$\frac{d\mathcal{C}_k}{dt} = -2\mathcal{C}_k + \gamma[\mathcal{C}_{k-1} + \mathcal{C}_{k+1}]. \quad (\text{II.23})$$

Note how Eq. (II.23) is identical in shape to the one for the expectation value in equation Eq. (II.18) with the change of variables  $t' = 2t$ , and will have, thus, similar solutions. The steady solutions of equation Eq. (II.23) can be found in the same way, with the ansatz  $\mathcal{C}_k = \zeta^{|k|}$ , and again,  $\zeta = \tanh \beta J$ . Note how these, for  $k > 0$ , can be written the following way,

$$\mathcal{C}_k = e^{-k/\xi}, \quad \xi := [\ln(\coth \beta J)]^{-1}, \quad (\text{II.24})$$

as one obtains for the equilibrium  $d = 1$  Ising chain correlation function. In order to find general solutions, one needs to find the proper linear combinations of the already known solutions, Eq. (II.20), for an arbitrary initial condition verifying that  $\mathcal{C}_k(0) = \delta_{k,0}$  since spins are initially uncorrelated for a random initial configuration and  $\mathcal{C}_0(t) = 1, \forall t$ , and add to the dynamical behaviour

the homogeneous, stationary, solution  $\zeta^{|k|}$ . The general solutions for  $k > 0$  become [12, 14],

$$\mathcal{C}_k = \zeta^k + e^{-2t} \sum_{m=-\infty}^{\infty} \mathcal{C}_m(0) I_{k-m}(2\gamma t). \quad (\text{II.25})$$

Note how the solutions in equations Eq. (II.22, II.25) can be generalized by means of fixing  $\langle \sigma_0 \rangle = 0$  instead, a more complete description can be found in [12, 14].

Both the MF solutions and the dynamical and steady behaviour of a  $d = 1$  Ising chain, with reciprocal interactions, are well known. In the following sections we will try to generalize these two when the reciprocal interactions between spins are replaced by non-reciprocal ones. The main goal is understanding what happens when we introduce an asymmetry of the coupling matrix through spin dependence. The lack of a properly defined Hamiltonian only allows the stochastic approach, for which this section will be essential. The results obtained for a generally asymmetric  $J_{ij}$  should return the results above when making the proper limit to make  $J_{ij}$  symmetric, the reciprocal limit. In order to see how, we will systematically compare the results obtained in the following sections with the ones reviewed in this one.

### III. NON-RECIPROCAL ISING MODEL

#### A. General Formulation

Consider now that the coupling matrix separates into a symmetric part and an asymmetric one,  $J_{ij} = J_{ij}^s + J_{ij}^a$ , with  $J_{ij}^s = J_{ji}^s$  but  $J_{ij}^a \neq J_{ji}^a$ . As a consequence, the coupling matrix  $J_{ij}$  will not be symmetric anymore, making the interactions between spins, generally, not reciprocal. Let's also consider that the competition between the symmetric part and the asymmetric one is governed by a single parameter  $\Delta$ , such that  $J_{ij}^a = \Delta \varrho_{ij}$  with  $\varrho_{ij} \neq \varrho_{ji}$ . We will at first make the assumption that the asymmetric part momentary depends on the spin configuration,  $\varrho_{ij} = \varrho_{ij}(\boldsymbol{\sigma})$ . This assumption is done since we are interested in studying what happens when the symmetry of the interaction is broken because it depends on the intrinsic state of each spin (e.g birds flocking, interaction among species).

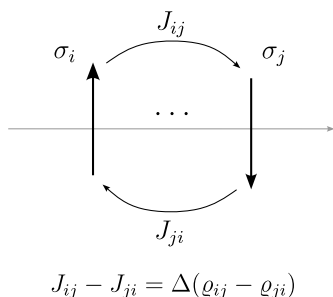


FIG. 2: Scheme showing the symmetry breaking of the interaction between spins for the general model considered. Note how the symmetry breaking is controlled by  $\Delta$ .

Since the definition of a Hamiltonian is ambiguous, a dynamic approach needs to be taken. We take as starting point the kinetic Ising model and, particularly, the local field (see Eq. (II.5)) governing the spin flip dynamics [5, 6], now with coupling matrix  $J_{ij} = J_{ij}^s + \Delta \varrho_{ij}$ . The local field governing the spin flip rate of spin  $\sigma_i$  becomes, thus,

$$h_i = h_0^i + \sum_{j=1}^N J_{ij}^s \sigma_j + \Delta \sum_{j=1}^N \varrho_{ij} \sigma_j, \quad (\text{III.1})$$

where the term including  $J_{ij}^s$  represents the reciprocal part of the interactions, which allows for a Hamiltonian description, and the term including  $\varrho_{ij}$  is the one breaking the symmetry, which makes the Hamiltonian approach ambiguous. We say, then, that the field  $h_i$  separates into a symmetric part and an asymmetric one. The strong non-linearity of the hyperbolic tangent term in the rates (Eq. (II.4)) makes finding dynamical equations hard in general, and so, one is forced to consider simpler cases, for instance, spin lattices up to first neighbours and FC models. In the following subsections we will consider FC models which include symmetry breaking of  $J_{ij}$ .

#### B. Methodology

##### 1. A Fully Connected Model

Let us now consider a FC model and  $h_0^i = 0$ . We are going to set the symmetric part to be the usual FC Ising model coupling matrix,  $J_{ij}^s = J(1 - \delta_{ij})$  and consider a general asymmetric part  $\varrho_{ij}$  with zeros in the diagonal,  $\varrho_{ii} = 0$ . The field  $h_i$  is again a global one. It is useful to define the field attributed to the reciprocal coupling,  $h_s^i = J \sum_{j \neq i} \sigma_j$ . In this case, studying the dynamics with the spin flip rates in equation Eq. (II.4) is still hard due to the above mentioned non-linearity.

In order to simplify the problem we can consider that  $\Delta$  represents small deviations with respect to  $J$ . This means that the symmetric part of the field,  $h_s^i$ , has a bigger contribution to the global field,  $h_i$ . Using perturbation theory for  $|\Delta| \ll J$  we can make the problem easier to tackle, since we already know the behaviour for  $\Delta = 0$ . Note how even if the asymmetric part of  $J_{ij}$  has a smaller contribution, the way the symmetry is broken can happen in multiple ways, since  $\varrho_{ij}$  can take any shape.

##### 2. The $|\Delta| \ll J$ Limit

The  $|\Delta| \ll J$  limit can be taken by expanding the hyperbolic tangent term,  $\tanh(\beta h_s^i + \beta \Delta \sum_j \varrho_{ij} \sigma_j)$ , around  $\Delta = 0$  at a given temperature,  $\beta$ , in the rates in equation Eq. (II.4) up until first order. The rates now read

$$\omega(\sigma_i, \Delta) = \omega^0(\sigma_i) + \delta\omega_i \Delta + \mathcal{O}(\Delta^2), \quad (\text{III.2})$$

where  $\omega^0(\sigma_i) = \frac{1}{2}[1 - \sigma_i \tanh \beta h_s^i]$  is the spin flip rate of the FC Ising model, Eq. (II.11), and where

$$\delta\omega_i = -\frac{\beta\sigma_i}{2} \left( \sum_{j=1}^N \varrho_{ij} \sigma_j \right) \text{sech}^2 \beta h_s^i. \quad (\text{III.3})$$

Note how by setting  $\Delta = 0$ ,  $\omega(\sigma_i, 0) = \omega^0(\sigma_i)$ , thus recovering the FC reciprocal Ising model spin flip rates, as expected. Now, the dynamic equation for the expectation value, Eq. (II.8), splits into two, since  $\langle \sigma_i \omega(\sigma_i, \Delta) \rangle = \langle \sigma_i \omega^0(\sigma_i) \rangle + \Delta \langle \sigma_i \delta \omega_i \rangle + \mathcal{O}(\Delta^2)$ . The first term including  $\omega^0(\sigma_i)$  has already been studied in section Sec. II A. Again, by defining the magnetization  $m = (1/N) \sum_i \sigma_i$ , we will have  $h_s^i \approx NJm$ , and

$$\langle \sigma_i \delta \omega_i \rangle = -\frac{\beta}{2} \operatorname{sech}^2 \beta NJm \sum_{j=1}^N \langle \varrho_{ij} \sigma_j \rangle, \quad (\text{III.4})$$

since  $\varrho_{ij}$  also depends on the spin state. Again, by neglecting the fluctuations and setting  $\langle \sigma_i \sigma_j \rangle = \langle \sigma_i \rangle \langle \sigma_j \rangle$ , we can build up the MF solutions of the dynamic equations. However, in order to perform the MF approximation, we need a definition of  $\varrho_{ij}$ . We will give two different examples, both with a physical meaning, for instance, as we will see, vision cones, see figures Fig. (5,9). As a first simplification, we will say that the asymmetric part of the coupling only depends on the state of a single spin,  $\varrho_{ij} = \psi(\sigma_i)(1 - \delta_{ij})$ .

### 3. Fully Connected Simulations

Besides the definition of possible models for which  $\varrho_{ij} = \psi(\sigma_i)(1 - \delta_{ij})$  and deriving their dynamical and static properties, we will perform simulations for each model to verify our results. We will study a system of  $N = 10^3$  spins, following the evolution of two different initially ordered states of spins pointing upwards +1 and downwards -1, and track the average temperature dependent steady configuration for different seeds.

The simulations were run as follows, we set an initially ordered state, of positive and negative magnetization, and we flip spins with the rates in equation Eq. (II.4), we let the system relax measuring the magnetization of the system until it reaches a stationary state, for  $N_s$  different seeds (repetitions), as shown in Fig. (3).

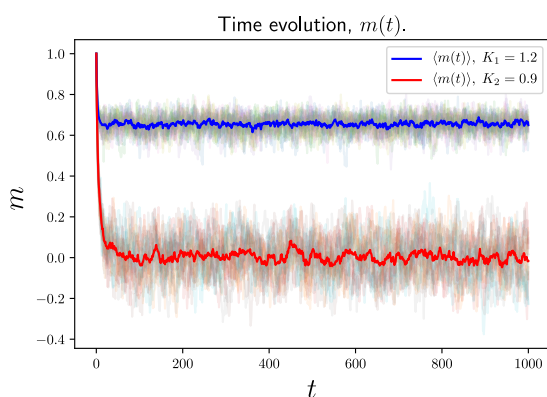


FIG. 3: Dynamical evolution of the magnetization for a fully connected Ising model of  $N = 10^3$  spins. The red and blue lines represent the average over  $N_s = 30$  seeds, for two different temperatures, below and above the critical temperature,  $K = 0.9$  and  $K = 1.2$ . Note how, again,  $K = \beta NJ$ .

The average magnetization for every repetition can be computed as

$$m(t) = \left\langle \frac{1}{N} \sum_{i=1}^N \sigma_i(t) \right\rangle, \quad (\text{III.5})$$

where  $\langle \dots \rangle$  denotes the ensemble average over different repetitions. Since the process is stochastic,  $m(t)$  in the stationary state fluctuates around a steady value, which is the value  $m(t)$  should converge to when making an ensemble average with  $N_s \rightarrow \infty$  seeds or repetitions. Looking at the dynamical evolution as shown in figure Fig. (3), we can find a range of times  $t \in (t_0, t_f)$  for which  $m(t)$  oscillates around a steady value, and then approximate this steady value by the time average over  $t \in (t_0, t_f)$  of  $m(t)$ ,  $t \in (500, 1000)$  in the case of Fig. (3). By doing so we can study the approximated steady state behaviour of  $m$  with temperature, and compare the results of the simulation with the numerical integration of the steady states through the self consistent equation  $\varphi(m; \beta) = 0$ , freezing the dynamics of  $m$  in equation Eq. (II.13), in order to draw the phase diagram (PD) as shown in figure Fig. (4).

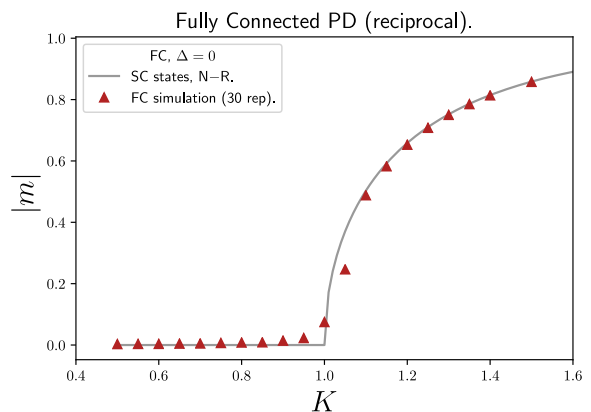


FIG. 4: Phase diagram showing the temperature dependence of the magnetization of the system. The dots represent the time and ensemble averaged steady state results of the simulations of a reciprocal fully connected Ising model and the solid lines the theoretical steady states solutions of the self consistent equation  $\varphi(m; \beta) = 0$ . Note how, again,  $K = \beta NJ$ .

The steady state solutions of the self consistent equations  $\varphi(m; \epsilon) = 0$ , where  $\epsilon$  represents any parameter of the system, such as temperature, will be integrated numerically using the Newton–Raphson (NR) method.

Besides studying the temperature dependence of the steady magnetization and the comparison with the numerically computed self consistent states, we will also study the susceptibility of the chain, defined as

$$\chi = K[\langle m^2 \rangle - \langle m \rangle^2], \quad (\text{III.6})$$

in order to study the critical temperature of the system.

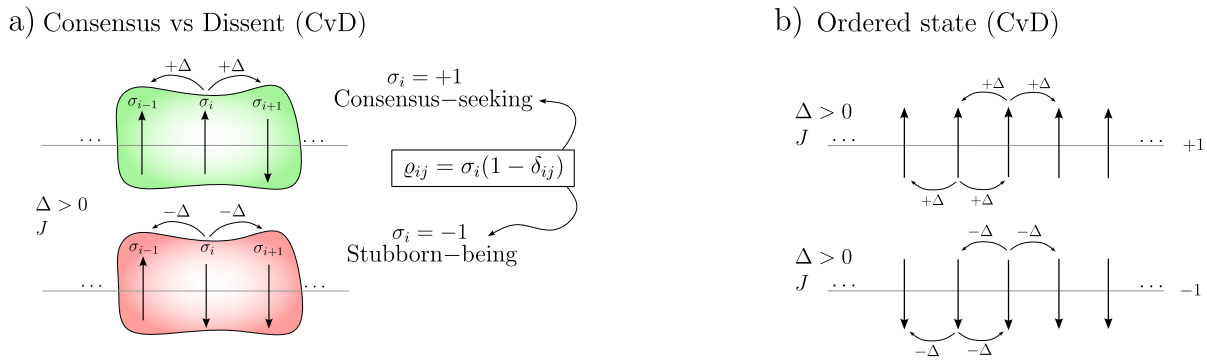


FIG. 5: Scheme showing: a) the definition of the Consensus vs Dissent model (CvD); b) how interactions along an ordered state of spins are reciprocal.

### C. Consensus vs Dissent Model (CvD)

Consider a system in which, besides the global ferromagnetic, consensus-seeking, coupling constant,  $J > 0$ , there exists two kind of agents: those who are willing to seek a stronger consensus, and the ones who are seeking the opposite, placing less relevance into finding consensus, which we will call stubborn-being. This is the case portrayed in figure Fig. (5. a)

In order to portray this consensus-seeking and stubborn-being competition we define  $\varrho_{ij} = \sigma_i(1 - \delta_{ij})$ , so that spins pointing up,  $\sigma_i = +1$ , will interact with coupling  $J + \Delta$ , and spins pointing down,  $\sigma_i = -1$ , with coupling constant  $J - \Delta$ , for  $\Delta > 0$ . Note how  $\Delta < 0$  just inverts the order of these, making upwards pointing spins stubborn and downwards pointing spins consensus-seeking. Note also how, spin pairs of the same sign interact reciprocally, while spin pairs with opposite sign interact non-reciprocally in this model. In the case of considering  $|\Delta| \ll J$ , although these interactions are generally not reciprocal, they are still of ferromagnetic nature, since  $J \pm \Delta > 0$ . Note how in any ordered state, spin interactions become reciprocal, Fig. (5.b).

Given now the definition of  $\varrho_{ij}$ , we can perform the MF approximation on the term in equation Eq. (III.4), for which now  $\langle \varrho_{ij} \sigma_j \rangle = (1 - \delta_{ij}) \langle \sigma_i \sigma_j \rangle \approx (1 - \delta_{ij}) \langle \sigma_i \rangle \langle \sigma_j \rangle$ , and, as a consequence,  $\sum_j \langle \varrho_{ij} \sigma_j \rangle \approx N \langle \sigma_i \rangle m$ . We can combine the term in equation Eq. (III.4) and the one corresponding to the symmetric part and find the evolution equation for  $\langle \sigma_i \rangle$ , as we did in equation Eq. (II.12). We can afterwards divide by  $N$  both sides, and sum over all spins, to find the equation for the magnetization  $m$ , which reads

$$\frac{dm}{dt} = -m + \tanh(Km) + Kqm^2 \operatorname{sech}^2(Km), \quad (\text{III.7})$$

where we have defined  $K = \beta NJ$  and  $q = \Delta/J$ . Here,  $q$  represents the relative strength of  $\Delta$  with respect to  $J$ , such that in the limit  $|\Delta| \ll J$ ,  $|q| \ll 1$ . Note how, again, we will define  $dm/dt := \varphi(m; K, q)$ , so that the right hand side of Eq. (III.7) is just  $\varphi(m; K, q)$ . The

stationary states will then be given by the self consistent equation  $\varphi(m; K, q) = 0$ . In figure Fig. (6) we represent  $\varphi(m; K, q)$  for different values of  $K$  and  $q$ , in order to show the appearance of non-zero self consistent states as well as the numerical solutions of these for different values of  $K$  and  $q$ , found using the NR method. One can see how, contrarily of what happened for the reciprocal case, the positive,  $m_+^*$ , and negative,  $m_-^*$ , branch are not symmetric, and the critical temperature changes with  $q$ .

Note how taking the reciprocal limit,  $\Delta = 0$ , such that  $q = 0$ , Eq. (III.7) reduces to the Ising MF dynamical equation for the magnetization,  $m$ , Eq. (II.13). We know that, in this case, the critical point is  $K_c = 1$ . For  $q \neq 0$ , there may be a critical point for which the limit  $q = 0$  returns the well known critical point of the MF Ising model,  $K_c = 1$ . With this in mind we can expand  $\varphi(m; K, q)$  around  $m = 0$ , so that the self consistent equation  $\varphi(m; K, q) = 0$  reads  $m \approx Km + Kqm^2 - \frac{1}{3}K^3m^3 + \mathcal{O}(m^4)$ . The non-zero solutions of this are

$$m_{\pm}^*(K, q) = \frac{1}{2} \left[ \frac{3q}{K^2} \pm \sqrt{\frac{9q^2}{K^4} + \frac{12(K-1)}{K^3}} \right]. \quad (\text{III.8})$$

Note how  $m_{\pm}^*(K, 0) \sim \pm \sqrt{3(K-1)}$ , recovering the Ising model's MF solutions close to the critical point  $K_c = 1$ . The critical point, if any, comes from studying the existence of non-zero solutions, which relies on the sign of the term in the square root. The roots of the term in the square root are  $K_q = \frac{1}{2}[1 \pm \sqrt{1 - 3q^2}]$ . Note how the solution with sign  $-$  is not physical since when  $q = 0$ , it returns  $K_c = 0$ . Before any further comments on the critical point, one can see how  $m_{\pm}^*(K = 1, q) = \frac{1}{2}(3q \pm 3|q|)$ . This tells us that when  $q > 0$ ,  $m_+^* = 3q$  and  $m_-^* = 0$ , while the opposite happens when  $q < 0$ . This portrays a broken symmetry of the positive and negative steady solutions of equation Eq. (III.7). The critical temperature is separated into two, the positive branch and the negative branch's. Furthermore, when the term in the square roots is identically 0, for small  $q$  (as intended),  $m_+^* \sim q$ , since  $K_q \approx 1$ , which portrays a discontinuity in the steady state solutions.

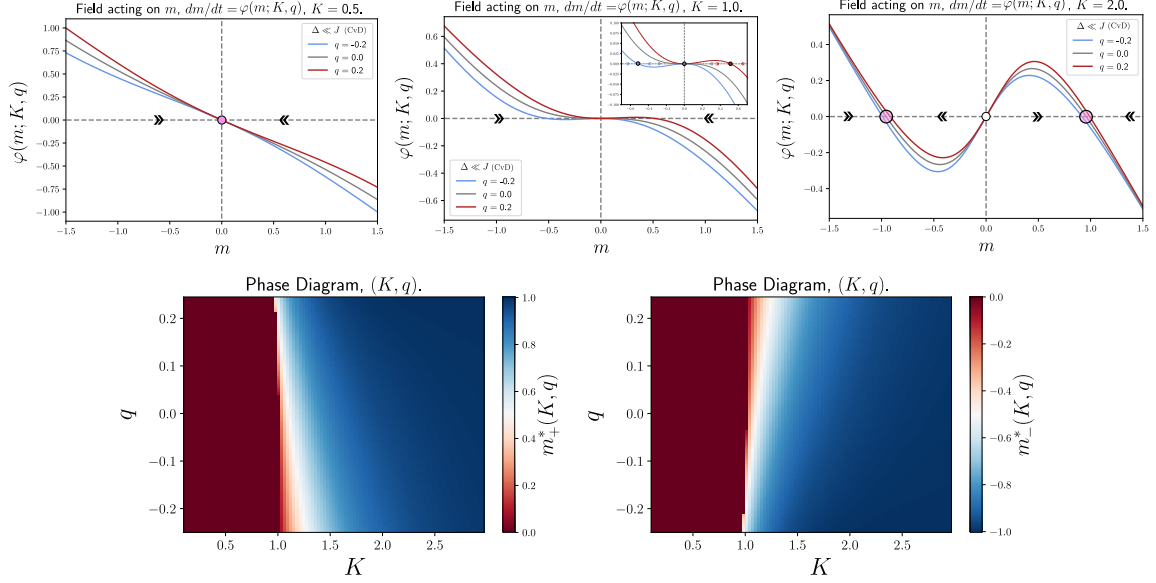


FIG. 6: Top:  $\varphi(m; K, q)$  for different values of  $q$  and  $K$ , for the CvD model, is shown. Note how the intersection with the  $m$  axis,  $\varphi(m; K, q) = 0$ , represent the steady solutions, fixed points, of the dynamic equation for  $m$ , with their stability also drawn. Bottom: heatmaps showing the stable solution of the self consistent equation  $\varphi(m; K, q) = 0$  for different values of  $K$  and  $q$ . Note how the positive branch,  $m_+^*$ , represents the positive steady state solutions, that is why the colorbar goes from 0, in red when  $|m| = 0$ , to 1, in blue, when  $|m| = 1$ , while the negative branch,  $m_-^*$ , represents the negative solutions, so that the colorbar goes from  $-1$  in blue when the system is magnetized, to 0, when there is no magnetization.

Expanding the self consistent equation for small  $m$  is justified, since around  $K = 1$ , both branches are small,  $m_{\pm}^* = \frac{1}{2}(3q \pm 3|q|)$ , for  $|q| \ll 1$ . Note how  $m_{\pm}^*(K_q, q) = 3q/2K_q^2$ . Since  $m_+^* \geq 0$  and  $m_-^* \leq 0$  represent the positive and negative solutions of the magnetization,  $K_q$  can only be critical temperature of  $m_+^*$  when  $q > 0$ , since  $m_+^*(K_q, q) > 0$  but  $m_-^*(K_q, q) > 0$ , which is a contradiction. In fact,  $m_-^* = 0$  is the stable solution of the negative branch at  $K_q$ , the non-zero stable solution  $|m_-^*| \neq 0$  appears at  $K_c = 1$ . The opposite happens when considering  $q < 0$ , and, thus, the critical temperatures read,

$$K_q^+ = \begin{cases} \frac{1}{2} [1 + \sqrt{1 - 3q^2}] & \text{if } q > 0 \\ 1 & \text{if } q \leq 0, \end{cases} \quad (\text{III.9})$$

$$K_q^- = \begin{cases} 1 & \text{if } q \geq 0 \\ \frac{1}{2} [1 + \sqrt{1 - 3q^2}] & \text{if } q < 0. \end{cases} \quad (\text{III.10})$$

Again, the reciprocal limit  $q = 0$  returns expected results. It is important to note how the negative and positive branch are now not symmetric for a given  $q$ , see Fig. (7, a). However, the solutions interchange when changing the sign of  $q$ ,  $m_{\pm}^*(q) = -m_{\mp}^*(-q)$ , the positive branch for  $q > 0$  has the shape of the negative one when  $q < 0$ , and so on. Note how  $K_q^{\pm} \leq 1$  for any  $q$  and how the steady state solutions at a given temperature  $K > 1$  have different modulus,  $|m_+^*(K, q)| \neq |m_-^*(K, q)|$ .

In figure Fig. (7) we show the discontinuity in  $m_+^*$  for  $q = 0.2$  while  $m_-^*$  remains continuous, showing the numerically obtained self consistent states close to the critical temperatures in equations Eq. (III.9, III.10) as well

as a comparison of the approximated critical temperature  $K_q^+$  for small  $m$  and the numerically integrated after finding the self consistent states of the positive branch,  $m \geq 0$  for  $q \in (-0.2, 0.2)$ .

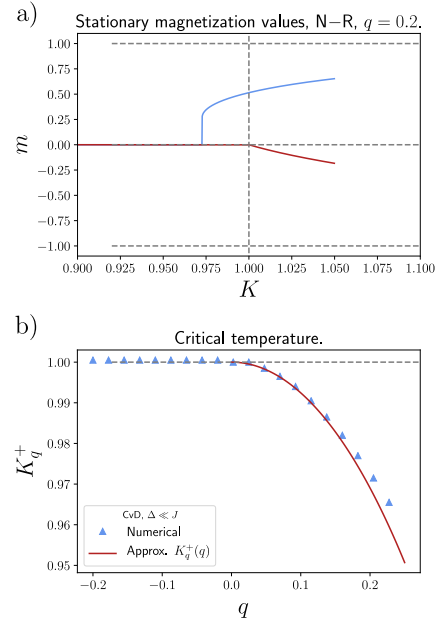


FIG. 7: a) Self consistent states of the CvD model found using the NR method for  $q = 0.2$ , showing how the positive branch presents a discontinuity while the negative branch remains continuous; b) Comparison between the numerically extracted critical temperature of the positive branch and the approximated one  $K_q^+$  for small  $m$ .

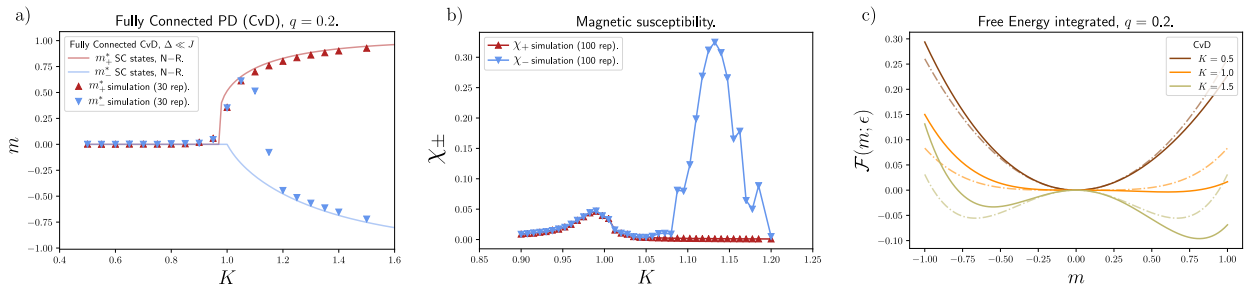


FIG. 8: a) Steady states of both positive (red) and negative branch (blue) computed through a simulation of  $N = 10^3$  spins and  $N_s = 30$  seeds for different values of  $K$  and  $q = 0.2$ ,  $J = 1$  compared to the self consistent states numerically found using the NR method; b) Magnetic susceptibility of both branches for different values of  $K$  around the critical temperatures, for  $N_s = 10^2$  seeds; c) Model's free energy for small  $m$  compared to the MF Ising free energy for different values of  $K$  (dashed).

Having explored the dynamical and static behaviour of  $m$  for  $|q| \ll 1$ , we can study the existence of a free energy like object,  $\mathcal{F}$ , governing the dynamics of  $m$ . Just as done in section Sec. (II A), we can interpret the right hand side of equation Eq. (III.7),  $\varphi(m; K, q)$ , as  $-\partial\mathcal{F}/\partial m$ . This can be understood as supposing that  $m$  evolves through the minimization of  $\mathcal{F}$ , which in the equilibrium case represents the mean field free energy of the system. In this case, since  $|q| \ll 1$ , spins, regardless of their state, generally interact non-reciprocally but ferromagnetically, since both  $J \pm \Delta$  are positive quantities. One hence can expect that the ferromagnetic order will still play a fundamental role. We can suppose that the steady state solutions come through a minimization principle. The free energy of the system for small  $m$  reads

$$\begin{aligned} \mathcal{F} = \mathcal{F}_0(K) - \frac{1}{2}(K-1)m^2 - \frac{1}{3}Kqm^3 \\ + \frac{1}{12}K^3m^4 + \mathcal{O}(m^5). \end{aligned} \quad (\text{III.11})$$

Note how, the last one becomes the MF free energy of the Ising model when taking the reciprocal limit  $q = 0$ , since the odd powers of  $m$  vanish. The presence of odd powers of  $m$  in the free energy signals lack of  $\mathbb{Z}^2$  symmetry of the chain. This is easy to understand since the rates are not spin inversion,  $\sigma_i \rightarrow -\sigma_i \forall i$ , invariant, and the responsible for this is the spin state dependence of the coupling matrix  $J_{ij}$ . The free energy has two minima representing both the positive and negative branch of the steady solutions of Eq. (III.7). The non-zero positive solutions  $m_+^*$  appear as a minimum of  $\mathcal{F}$  for  $K > K_q^+$ , while the negative ones for  $K > 1$  when  $q > 0$ . Note how the position of the minima represent different magnetization states,  $|m_-^*| \neq |m_+^*|$ , and have different free energies, thus signaling metastability.

In figure Fig. (8) we show several aspects regarding what we have mentioned so far. In figure Fig. (8.a) we show the steady state behaviour after  $N_s = 30$  repetitions, for different values of  $K$ , of a simulation as explained in section Sec. (III B 3) using the rates defined in equation Eq. (II.4), with the field  $h_i$  in equation Eq. (III.1) and  $\varrho_{ij} = \sigma_i(1 - \delta_{ij})$ , for  $q = 0.2$ ,  $J = 1$ . We compare the time and ensemble averaged simulations with

the numerical integration of solutions of the self consistent equation  $\varphi(m; K, q) = 0$  in the  $|\Delta| \ll J$  limit. As we can see, a broken symmetry between the positive and negative branch of the steady solutions for high  $K$ , low  $T$ , is also present in the simulations, which fit almost perfectly the self consistent states. The disordered phase  $m = 0$  is the stable one for low  $K$ , high  $T$ , as expected. Note, however, how close to the critical point of the positive branch, the negative branch of the simulations follows the behaviour of the positive one until certain point, for which it starts returning back to the behaviour of the negative branch solutions of the self consistent equation. In this range of  $K$ , some repetitions find as steady state the positive branch of the solutions, while some other the negative one, until  $K^* \approx 1.2$  for which only the negative solutions are found. These jumps between branches may be a consequence of the metastability mentioned before.

In order to understand why this happens, we plot in figure Fig. (8.b) the susceptibility  $\chi_{\pm}$  of each simulated branch (+ for positive, - for negative) for different values of  $K$ . We can see how the positive branch of the simulations only shows one peak, the one around its critical temperature, while the negative shows two, one corresponding to the positive branch like behaviour and then another one for its relaxation, back again, to the negative branch like behaviour. In figure Fig. (8.c) we show the integrated free energy for different  $K$  and the corresponding Ising model's MF free energy (dashed). As we can see, the  $\mathbb{Z}^2$  symmetry that appears in the Ising model's MF free energy is now broken. For instance, for  $K = 0.5$  the only minimum is still the disordered phase, although now the free energy pushes the negative branch stronger towards  $m = 0$  than it does for the positive branch, since it is way steeper for  $m < 0$ . For  $K = 1.0$  we can see how there is no minima for  $m < 0$  while there is for  $m > 0$ , the positive branch appears as a stable phase before the negative one does. Lastly, for  $K = 1.5$  we can see how even if there is two minima, they appear at different magnetizations depending on the branch,  $|m_-^*| < |m_+^*|$ , and how the free energy of the positive branch is always smaller than the negative branch's,  $\mathcal{F}(m_+^*; K, q) < \mathcal{F}(m_-^*; K, q)$  for  $K > 1$  and  $q > 0$ . The behaviour is analogous for  $q < 0$ , interchanging the positive and the negative branches.

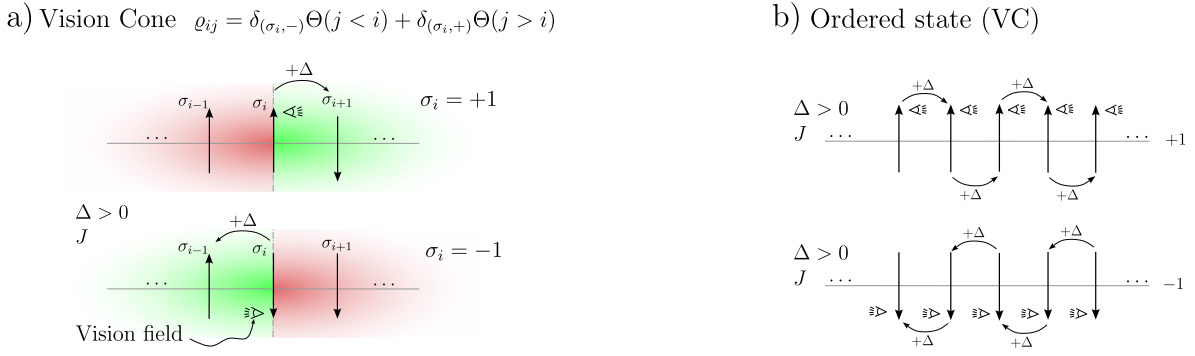


FIG. 9: Scheme showing: a) the definition of the Vision Cone model (VC); b) how interactions along an ordered state of spins are, in this case, non-reciprocal.

#### D. Vision Cone Model (VC)

Let us now consider a system in which, again, besides the global ferromagnetic coupling constant,  $J > 0$ , the symmetry is broken by spin state dependence. Imagine the situation shown in figure Fig. (9.a), for which spins have an intrinsic vision field that directly influences the way they interact. This kind of interaction is fairly common in bird flocking and fish banks, and has also been studied using the XY model [16].

In order to portray the vision field effect breaking the symmetry of the coupling matrix we define  $\varrho_{ij} = \delta_{(\sigma_i,-)}\Theta(j < i) + \delta_{(\sigma_i,+)}\Theta(j > i)$ , where  $\Theta(\circ)$  is the Heaviside step function, such that  $\Theta(j < i) = 1, \forall j < i$  while  $\Theta(j < i) = 0, \forall j > i$  and so on, and where  $\delta_{(\sigma_i,\pm)}$  is the Kronecker delta of states  $\pm 1$  of the spin  $\sigma_i$ . Note how  $\varrho_{ii} = 0$ . This can be interpreted as if spins prioritized the spins they have on their right. If a spin  $\sigma_i$  is pointing upwards, it will prioritize spins to its right,  $\sigma_j$  with  $j > i$  and if it is pointing downwards, it will, analogously, prioritize spins  $\sigma_j$  now with  $j < i$ . The coupling between spins will become  $J + \Delta$  and  $J$  to its right and left depending on their state, and, hence, interactions will be generally not reciprocal. Note how in any ordered state, interactions are not reciprocal, Fig. (9.b).

Again, given the definition of  $\varrho_{ij}$  we can perform the MF approximation of  $\langle \varrho_{ij}\sigma_j \rangle$  to find the term in equation Eq. (III.4) in order to afterwards compute the dynamical equation for  $\langle \sigma_i \rangle$  and, eventually, the one for the magnetization  $m$ . The result reads (see Appendix B),

$$\begin{aligned} \frac{dm}{dt} &= -m + \tanh(Km) \\ &+ \frac{1}{2}Kqm[1 + m(1 - 2z)] \operatorname{sech}^2(Km), \end{aligned} \quad (\text{III.12})$$

where, again,  $K = \beta NJ$ ,  $q = \Delta/J$  and now  $z$  represents a MF parameter, the fraction of prioritized spins. Note how  $z$  appears from the definition of  $\varrho_{ij}$ . For instance, considering a chain, the definition of  $\varrho_{ij}$  divides the system into two, the prioritized fraction by spin  $\sigma_i$  and the

rest. A chain then is divided into two,  $j < i$  and  $j > i$ . Hence, see Appendix B,  $z$  naturally appears as the relative position of  $\sigma_i$  on the chain, such that when taking the limit  $N \rightarrow \infty$  and considering spins as identical,  $z$  stops having geometrical sense, and we shall interpret it as the fraction of prioritized spins of a single spin  $\sigma_i$ . This interaction is naturally non-reciprocal: each spin identically prioritizes a fraction of spins  $z$  of the system. The prioritized spins don't need to be the same between different spins. A spin  $\sigma_i$  may have spin  $\sigma_j$  in its vision field, but  $\sigma_i$  may not be in  $\sigma_j$ 's. Note how in this MF scenario, a spin  $\sigma_i = +1$  prioritizes a fraction  $z$  by  $+\Delta$  while a spin  $\sigma_i = -1$  prioritizes a fraction  $1 - z$ . This can be understood as a redefinition of  $\varrho_{ij}$  without geometry, in which  $z$  and  $1 - z$  play the role of the Heaviside step functions.

We can again define the right hand side of equation Eq. (III.12) as  $\varphi(m; K, q, z)$ . The stationary states will again be given by the self consistent equation  $\varphi(m; K, q, z) = 0$ . In figure Fig. (10) we show, again, the dynamical field  $\varphi(m; K, q, z)$  for different values of  $K, z$  and  $q = \{-0.2, 0.0, 0.2\}$  in order to show the appearance of non-zero solutions of the self consistent equation.

One can see how  $q = 0$  returns the expected MF Ising dynamical map, hence returning the MF stationary, equilibrium, states of the Ising model. Note, however, how now  $z$  also plays a fundamental role;  $\varphi(m; K, q, z)$  is anti-symmetric with respect to an  $m$  inversion,  $m \rightarrow -m$  when  $z = 1/2$ ,  $\varphi(m; K, q, 1/2) = -\varphi(-m; K, q, 1/2)$ . This makes sense since in this situation, regardless of their state, spins prioritize by  $+\Delta$  a fraction  $z = 1/2$ , and thus any  $m$  is driven, in both branches, with the same strength to its fixed point. The  $z \neq 1/2$  situation is a biased one, since a bigger or smaller fraction of spins is prioritized depending on the state of the spin. Even if the case  $z = 1/2$  may give symmetric self consistent states for the negative and positive branch, it does not represent the Ising model, since, again, interactions are generally not reciprocal. This is easily seen in equation Eq. (III.12), for which even if  $z = 1/2$ ,  $q$  has a contribution to the dynamics of  $m$ .

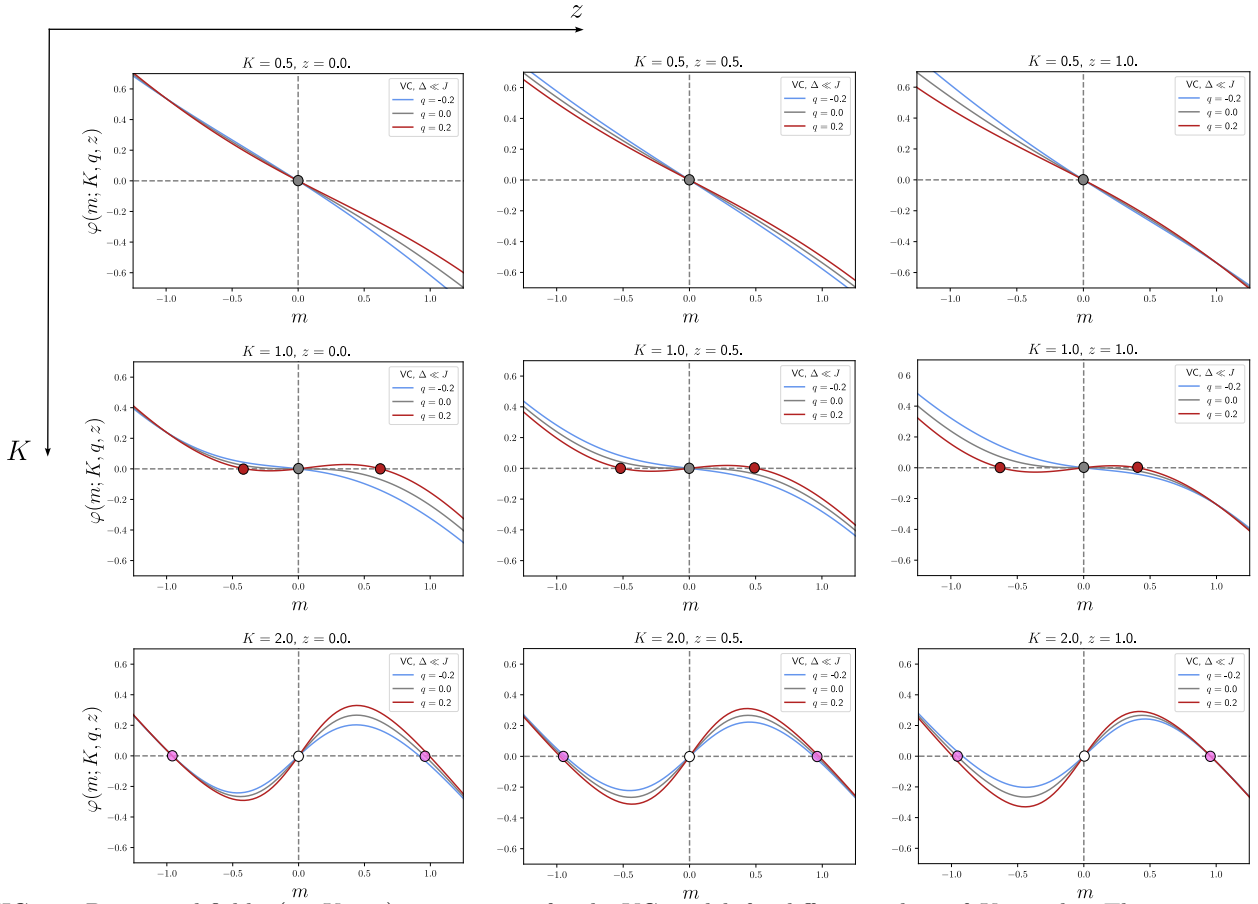


FIG. 10: Dynamical field  $\varphi(m; K, q, z)$  acting on  $m$ , for the VC model, for different values of  $K, z$  and  $q$ . The intersections with the  $m$  axis  $\varphi(m; K, q, z) = 0$  represent stationary solutions, stable or unstable, of  $m$ .

In figure Fig. (11) we show the numerically found solutions of the self consistent equation  $\varphi(m; K, q, z) = 0$  for different values of  $K, q, z$  in the shape of heatmaps. By looking at the heatmaps in space  $(K, q)$  we can see again how the positive,  $m_+$ , and negative,  $m_-$ , branch's self consistent states are not symmetric, and how, again, the critical temperature changes. By looking at the ones in the  $(q, z)$  space at  $K = 1$ , which represents the critical

temperature of the MF Ising model, it can clearly be seen how  $z_c = 1/2$  divides the system into two, and how, again, the positive and negative branch are not symmetric.

Since, again, the reciprocal limit  $q = 0$  returns the MF dynamics of the Ising model, we expect the critical point be close to  $K \approx 1$ . By means of a Taylor expansion of the self consistent equation  $\varphi(m; K, q, z) = 0$  for small  $m$ , the non-zero self consistent states become

$$m_{\pm}^*(K, q, z) = \frac{1}{2} \left[ \frac{3}{2} \frac{q(1-2z)}{K^2(1+3q/2)} \pm \sqrt{\frac{9}{4} \frac{q^2(1-2z)^2}{K^4(1+3q/2)^2} + \frac{12[K(1+q/2) - 1]}{K^3(1+3q/2)}} \right]. \quad (\text{III.13})$$

As expected,  $q = 0$  returns the Ising model's MF solutions close to the critical point  $m_{\pm}^* \sim \pm \sqrt{3(K-1)}$ . Note how the solutions in Eq. (III.13) are symmetric when evaluated at  $z = 1/2$ , with a  $q$  dependent critical temperature. The critical temperature of both branches is hidden in the term in the square root.

The self consistent states in Eq. (III.13) may also show a discontinuity. Note how when the term in the square root is 0,  $m_{\pm}^* \sim q(1-2z)/K^2(1+3q/2)$ . Im-

posing that  $m_+^* \geq 0$  and  $m_-^* \leq 0$ , implies that  $m_{\pm}^* \sim q(1-2z)/K^2(1+3q/2)$  is only solution for the positive branch,  $m_+^*$ , when  $q > 0, z < 1/2$  or when  $q < 0, z > 1/2$  considering that in the  $|q| \ll 1$  limit  $1+3q/2 > 0$ , and can only be solution for the negative branch in the analogous cases, for the same reasons we discussed for the CvD model. In order to investigate the symmetry breaking of the positive,  $m_+^*$ , and negative,  $m_-^*$ , branches, we can use a trick like the one we used for the CvD model.

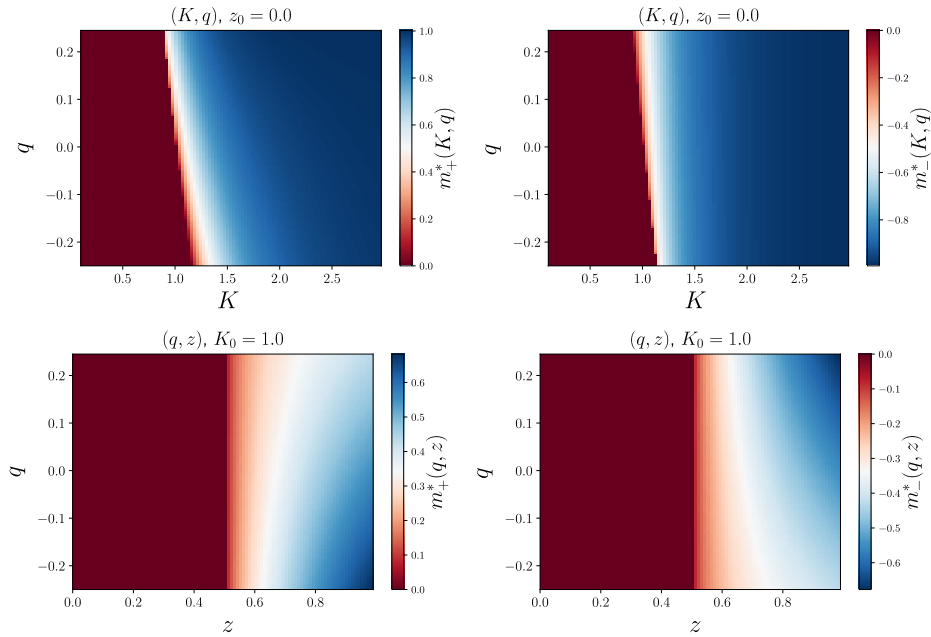


FIG. 11: Top: heatmaps showing the numerically found self consistent states of the positive,  $m_+^*$ , and negative,  $m_-^*$ , branch of the VC model,  $\varphi(m_\pm^*; K, q, z) = 0$ , in the  $(K, q)$  space, for  $z_0 = 0.0$ , using the NR method. Bottom: heatmaps showing the numerically found self consistent states of the positive and negative branch for the VC model in the space  $(q, z)$  for  $K = 1.0$ . Note how again the colorbars go from  $m_+^* \in (0, 1)$  and  $m_-^* \in (-1, 0)$  where red represents  $|m| = 0$ , and blue  $|m| = 1$ .

It can be seen how, in this case, along the line  $K(1 + q/2) - 1 = 0$ , the self consistent states take the shape  $m_\pm^* = \frac{1}{2}(\alpha \pm |\alpha|)$  where  $\alpha = \frac{3}{2}q(1 - 2z)/K^2(1 + 3q/2)$ . Again, when  $\alpha > 0$ , we will have that  $m_+^* = \alpha$  while  $m_-^* = 0$ , and when  $\alpha < 0$ , instead,  $m_+^* = 0$  while  $m_-^* = \alpha$ . This is similar to what happened in the CvD model. Actually, the line  $K(1 + q/2) - 1 = 0$  represents the critical temperature when  $z = 1/2$ , as we can see by plugging  $z = 1/2$  in equation Eq. (III.13), which reads  $K_q^{1/2} = \frac{1}{1+q/2}$ . The conditions  $\alpha > 0$  and  $\alpha < 0$  refer to the conditions  $q > 0, z < 1/2, q < 0, z > 1/2$  and  $q >$

$0, z > 1/2, q < 0, z < 1/2$ . This portrays the  $z$ -critical, with  $z_c = 1/2$ , behaviour seen in the  $(q, z)$  heatmaps in figure Fig. (11).

Considering now  $q > 0$  and the above mentioned behaviour regarding the continuity and the criticality at  $z_c = 1/2$ , we can study the behaviour of the critical temperature for any  $z$ . The roots of the term in the square root in equation Eq. (III.13) can be found. There's two roots, and just as we saw for the CvD model, the one with the negative sign shall be discarded since it returns  $K_c = 0$  when taking the reciprocal limit. We will have,

$$K_q^{z(+)} = \begin{cases} \frac{1}{2} \frac{1}{1+q/2} \left[ 1 + \sqrt{1 - \frac{3}{4} \frac{1+q/2}{1+3q/2} q^2 (1-2z)^2} \right] & \text{if } z < 1/2, q \geq 0 \\ \frac{1}{1+q/2} & \text{if } z \geq 1/2, q \geq 0, \end{cases} \quad (\text{III.14})$$

$$K_q^{z(-)} = \begin{cases} \frac{1}{1+q/2} & \text{if } z \leq 1/2, q \geq 0 \\ \frac{1}{2} \frac{1}{1+q/2} \left[ 1 + \sqrt{1 - \frac{3}{4} \frac{1+q/2}{1+3q/2} q^2 (1-2z)^2} \right] & \text{if } z > 1/2, q \geq 0. \end{cases} \quad (\text{III.15})$$

Note how the critical temperature for the case  $q \leq 0$  can be found by interchanging the positive branch and the negative branch of the last ones, Eqs. (III.14, III.15). Note also how, the reciprocal limit  $q = 0$  corresponds to the Ising model's critical temperature,  $K_c = 1$ .

In figure Fig. (13) we show the discontinuity mentioned above as well as a comparison of the numerically found critical temperature by an integration of the self consistent states of the positive branch and the approxi-

mated one for small  $m$ , Eq. (III.14), through the Taylor expansion of the self consistent equation.

Again, having studied the stationary behaviour of  $m$ , and since interactions, even if non-reciprocal, are still ferromagnetic when  $|q| \ll 1$ , we can make the same assumptions we made for the CvD model, and consider that the dynamics of  $m$  is governed by a minimization principle, thus identifying  $\varphi(m; K, q, z)$  with  $-\partial\mathcal{F}/\partial m$ .

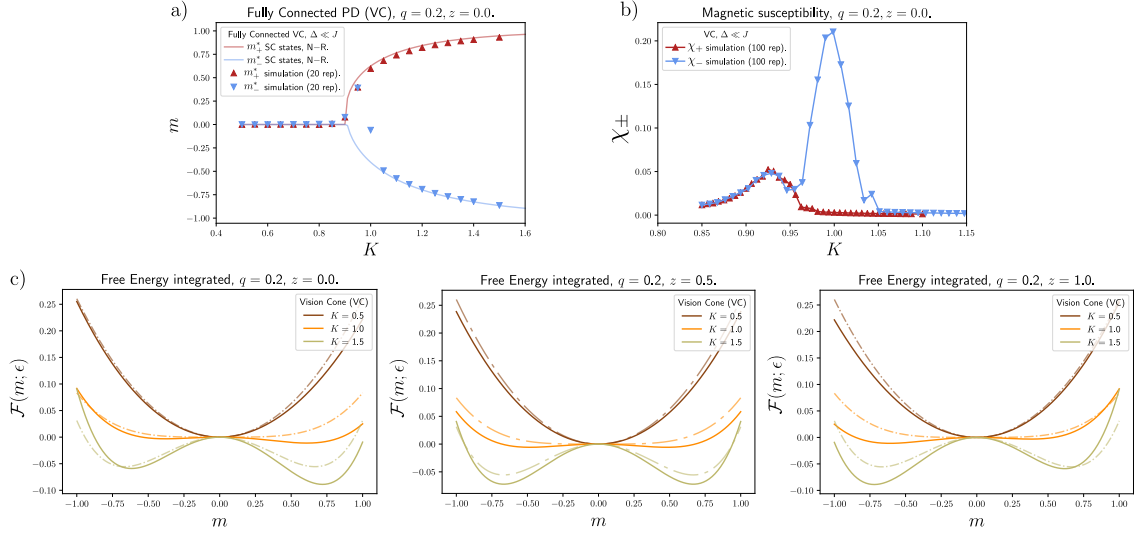


FIG. 12: a) Steady states of both positive,  $m_+^*$ , (red) and negative,  $m_-^*$ , (blue) branch obtained through a simulation of  $N = 10^3$  spins and  $N_s = 30$  repetitions for different values of  $K$  and  $q = 0.2, J = 1, z = 0.0$ , compared to the self consistent states (solid lines); b) Magnetic susceptibility of both branches for different values of  $K$  around the critical temperatures, now for  $N_s = 10^2$  repetitions; c) Model's free energy for small  $m$  compared to the MF free energy (dashed) for different values of  $K$ .

The free energy for small  $m$  reads in this case,

$$\mathcal{F} = \mathcal{F}_0(K) - \frac{1}{2} \left[ K \left( 1 + \frac{q}{2} \right) - 1 \right] m^2 - \frac{1}{6} K q (1 - 2z) m^3 + \frac{1}{12} K^3 \left( 1 + \frac{3q}{2} \right) m^4 + \mathcal{O}(m^5). \quad (\text{III.16})$$

Note how, again, the odd power terms vanish when either  $z = 1/2$  or  $q = 0$ . The Ising MF free energy, again, is recovered when taking the reciprocal limit  $q = 0$ .

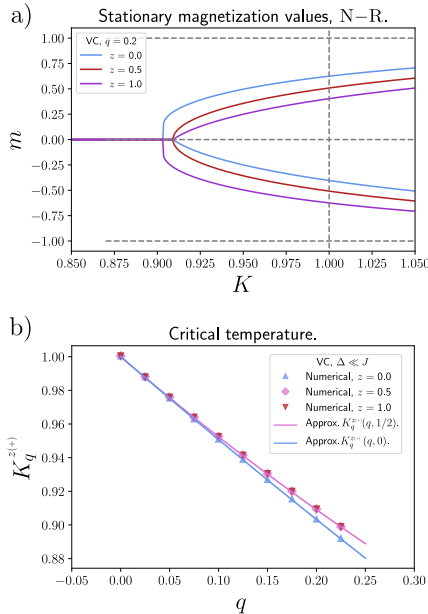


FIG. 13: a) Positive,  $m_+^*$ , and negative,  $m_-^*$ , stationary solutions for  $q = 0.2$  showing the discontinuities in  $m_{\pm}^*$  depending on  $z$ , while for  $z = 1/2$  they remain continuous and symmetric; b) Comparison of the numerically extracted critical temperature of  $m_+^*$  and the approximated one  $K_q^{z(+)}$ .

The presence of odd powers of  $m$  breaks the  $\mathbb{Z}^2$  symmetry. The case  $z = 1/2$  returns a  $\mathbb{Z}^2$  symmetric free energy, even if different from the Ising model's MF one. This is a consequence of the symmetry of both branches when  $z = 1/2$ , as seen in equation Eq. (III.13). A similar kind of behaviour is seen for the positive and negative branch, which are generically not symmetric. This asymmetry now depends on  $z$ .

This can easily be seen in figure Fig. (12). In figures Fig. (12.a,b) we show the steady state of a simulation of  $N = 10^3$  spins, just as done for the CvD model, now for  $N_s = 20$  seeds with  $q = 0.2, J = 1, z = 0.0$  and the self consistent states found for small  $q$ , as well as the susceptibility of both branches. We can see similar behaviour to the one observed in the case of the CvD model. The negative branch is found in the positive branch's mean field solution in some repetitions, in certain range of  $K$ , thus signaling, again, metastability.

The initially ordered  $-1$  spin configurations can land on the steady state solution of the positive branch: within some range of the temperature  $K$  some repetitions land on the positive branch's solution, usually more frequently for  $K < 1$ , and some land on the negative branch's instead, more frequently beyond  $K > 1$ . The represented dots, again, are the ensemble and time average of the found steady states throughout the simulation. In figure Fig. (12,c) we represent the model's free energy. We can clearly see again the asymmetry of the free energy, and how the wells have different depths, portraying hence metastability. For  $z = 1/2$ , as mentioned above, the odd powers of  $m$  disappear, and this can be seen since, in this case, the free energy seems to be symmetric, although it does not have the same exact shape of the Ising model's MF free energy. Note how the free energy for  $z = 1$  is just the reflection of the one for  $z = 0$ . This is related to the  $z = 1/2$  symmetric behaviour we mentioned above.

### E. Discussion

The results obtained for both the CvD and the VC model are remarkably similar. Even if in both models the reciprocity is broken since now the interactions are coupled to the state of each spin, they are notably different in nature. They still, however, share a great amount of properties: the existence of a discontinuous or first order phase transition in one of the branches of the steady solutions of the magnetization as well as the asymmetry of the positive and negative branches, which originates from the lack of  $\mathbb{Z}^2$  symmetry of the free energy, and the non-uniqueness of critical temperatures. This indicates that non-reciprocal models, in general, may present both discontinuities and lack of  $\mathbb{Z}^2$  symmetry as well. This lack of  $\mathbb{Z}^2$  symmetry through  $m \rightarrow -m$  inversions is a consequence of how the strength of the interaction changes with the state of the spins, since now, generally  $|J_{ij}(\sigma_i)| \neq |J_{ij}(-\sigma_i)|$ , and this can make ordering towards different magnetization states  $+1$  and  $-1$  of different strength.

### IV. NON-RECIPROCAL ISING CHAIN

Following what was done for the general formulation in section Sec. (III), consider now, instead, a  $d = 1$  chain of spins for which the symmetric part of  $J_{ij}$  vanishes,  $J_{ij}^s = 0$  for all  $i, j$ , such that only the asymmetric part  $J_{ij}^a = \Delta \varrho_{ij}$  remains. Just as we did in the previous section, we will consider that  $\varrho_{ij}$  depends on the configuration of spins but, however, now limited to first neighbours interactions. This means that  $\varrho_{ij}$  is only different from zero above and below the diagonal, which is also zero.

In this case, the rates in equation Eq. (II.4), taking again  $h_0^i = 0$ , read

$$\omega(\sigma_i) = \frac{1}{2} \left[ 1 - \sigma_i \tanh \left( \beta \Delta \sum_{j \in \langle i \rangle} \varrho_{ij} \sigma_j \right) \right], \quad (\text{IV.1})$$

where the sum is run over all the first neighbours of  $\sigma_i$ ,  $j \in \langle i \rangle$ . Again, one could try plugging these rates  $\omega(\sigma_i)$  into equations Eq. (II.8, II.9) and try to work out a way of finding the dynamic equations for the expected value  $\langle \sigma_i \rangle(t)$  and the correlation function  $\langle \sigma_i \sigma_j \rangle(t)$ . However, the non-linearity of the hyperbolic tangent term makes it hard. In order to make things simpler, one has to make a few assumption on how the matrix  $\varrho_{ij}$  looks like.

#### A. Constraints on $\varrho_{ij}$

In order to make the problem easier one can make a few assumption on how  $\varrho_{ij}$  looks like. Taking into account the property of the hyperbolic tangent we used while discussing the  $d = 1$  kinetic Ising chain in section Sec. (II.B),  $\tanh \varepsilon x = \varepsilon \tanh x$  when  $\varepsilon = 0, \pm 1$ , we can try to find simple definitions of  $\varrho_{ij}$  which make possible using the identity in order to simplify the rates.

As shown in Appendix. D, two simple definitions make this possible. The first one (Appendix. D.1) considers matrices  $\varrho_{ij}$  composed of 1 or  $-1$  above and below the

diagonal, that is, spin  $\sigma_i$  interacts with its nearest neighbours  $\sigma_{i \pm 1}$  with coupling  $\varrho_{i, i \pm 1} = \pm 1$ , for which, then  $\frac{1}{2} \sum_{j \in \langle i \rangle} \varrho_{ij} \sigma_j = 0, \pm 1$ . Hence, multiplying and dividing the argument of the hyperbolic tangent by two in equation Eq. (IV.1), the rates transform to

$$\omega(\sigma_i) = \frac{1}{2} \left[ 1 - \frac{\tilde{\gamma}}{2} \sigma_i \sum_{j \in \langle i \rangle} \varrho_{ij} \sigma_j \right], \quad \tilde{\gamma} = \tanh 2\beta \Delta. \quad (\text{IV.2})$$

Note how these coincide with the Ising chain spin flip rates in equation Eq. (II.17) when considering the symmetric case  $\varrho_{ij} = \delta_{i-1, j} + \delta_{i+1, j}$ , with coupling constant  $\Delta$ . By means of plugging the rates in equation Eq. (IV.2) and working out the algebra, the dynamic equations Eq. (II.8, II.9) read

$$\frac{d\langle \sigma_i \rangle}{dt} = -\langle \sigma_i \rangle + \frac{\tilde{\gamma}}{2} \sum_{k \in \langle i \rangle} \langle \varrho_{ik} \sigma_k \rangle, \quad (\text{IV.3})$$

$$\begin{aligned} \frac{d\langle \sigma_i \sigma_j \rangle}{dt} &= -2\langle \sigma_i \sigma_j \rangle + \frac{\tilde{\gamma}}{2} \left\langle \sigma_j \sum_{k \in \langle i \rangle} \varrho_{ik} \sigma_k \right\rangle \\ &\quad + \frac{\tilde{\gamma}}{2} \left\langle \sigma_i \sum_{\ell \in \langle j \rangle} \varrho_{j\ell} \sigma_\ell \right\rangle. \end{aligned} \quad (\text{IV.4})$$

Note how the expected values still include  $\varrho_{ij}$  since we will generally consider that it depends on the state of the spin and how, particularly, by means of setting again  $\varrho_{ij} = \delta_{i-1, j} + \delta_{i+1, j}$  we recover the dynamic equations of an Ising chain, Eq. (II.18, II.19). As we will see, the CvD model can be extrapolated to a  $d = 1$  spin chain to find dynamic equations of this type.

The second simple definition (Appendix. D.2) consists of considering matrices  $\varrho_{ij}$  which are made up of a 0 on one side of the diagonal and a  $\pm 1$  on the other. In this case spins  $\sigma_i$  will only be interacting with one of its neighbours, and the identity  $\sum_{j \in \langle i \rangle} \varrho_{ij} \sigma_j = \pm 1$  is verified. In this case, the spin flip rates transform to

$$\omega(\sigma_i) = \frac{1}{2} \left[ 1 - \tilde{\gamma} \sigma_i \sum_{j \in \langle i \rangle} \varrho_{ij} \sigma_j \right], \quad \tilde{\gamma} = \tanh \beta \Delta. \quad (\text{IV.5})$$

The dynamical equations of the expected value and the correlation function, in this case, read

$$\frac{d\langle \sigma_i \rangle}{dt} = -\langle \sigma_i \rangle + \tilde{\gamma} \sum_{k \in \langle i \rangle} \langle \varrho_{ik} \sigma_k \rangle, \quad (\text{IV.6})$$

$$\begin{aligned} \frac{d\langle \sigma_i \sigma_j \rangle}{dt} &= -2\langle \sigma_i \sigma_j \rangle + \tilde{\gamma} \left\langle \sigma_j \sum_{k \in \langle i \rangle} \varrho_{ik} \sigma_k \right\rangle \\ &\quad + \tilde{\gamma} \left\langle \sigma_i \sum_{\ell \in \langle j \rangle} \varrho_{j\ell} \sigma_\ell \right\rangle. \end{aligned} \quad (\text{IV.7})$$

Note how the the last two differ from the Ising chain's dynamical equations because now  $\varrho_{ij}$  also contains a zero to nearest neighbour level as well. This particular kind of definition will be useful for models like the VC model.

### B. Consensus vs Dissent Model (CvD)

The CvD model was defined as  $\varrho_{ij} = \sigma_i(1 - \delta_{ij})$  in the FC approach. For a  $d = 1$  spin chain this can be extrapolated by limiting  $\varrho_{ij}$  to nearest neighbour interactions, by setting  $\varrho_{ij} = \sigma_i(\delta_{i-1,j} + \delta_{i+1,j})$ . This means that spin  $\sigma_i$  interacts with its neighbours  $\sigma_{i\pm 1}$  with coupling  $\varrho_{i,i\pm 1} = \sigma_i$ . Generally speaking, again, interactions are not reciprocal and, now, they are generally not of ferromagnetic nature either, since  $\varrho_{i,i\pm 1}$  can be either positive or negative.

The CvD model's definition for a  $d = 1$  spin chain,  $\varrho_{i,i\pm 1} = \sigma_i$ , is of the first kind (Appendix. D1) as mentioned above; it consists of  $\pm 1$  elements above and below the diagonal. By means of plugging into equations Eq. (IV.3, IV.4) the definition of  $\varrho_{ij}$  for the  $d = 1$  spin chain CvD model, we have

$$\frac{d\langle\sigma_i\rangle}{dt} = -\langle\sigma_i\rangle + \frac{\tilde{\gamma}}{2}[\langle\sigma_i\sigma_{i-1}\rangle + \langle\sigma_i\sigma_{i+1}\rangle], \quad (\text{IV.8})$$

$$\begin{aligned} \frac{d\langle\sigma_i\sigma_j\rangle}{dt} = & -2\langle\sigma_i\sigma_j\rangle + \frac{\tilde{\gamma}}{2}[\langle\sigma_i\sigma_{i-1}\sigma_j\rangle + \langle\sigma_i\sigma_{i+1}\sigma_j\rangle] \\ & + \frac{\tilde{\gamma}}{2}[\langle\sigma_i\sigma_j\sigma_{j-1}\rangle + \langle\sigma_i\sigma_j\sigma_{j+1}\rangle], \end{aligned} \quad (\text{IV.9})$$

---


$$\frac{d\langle\sigma_i\rangle}{dt} = -\langle\sigma_i\rangle + \frac{\tilde{\gamma}}{2}[\langle\sigma_{i-1}\rangle + \langle\sigma_{i+1}\rangle] + \frac{\tilde{\gamma}}{2}[-\langle\sigma_i\sigma_{i-1}\rangle + \langle\sigma_i\sigma_{i+1}\rangle] \quad (\text{IV.10})$$

$$\begin{aligned} \frac{d\langle\sigma_i\sigma_j\rangle}{dt} = & -2\langle\sigma_i\sigma_j\rangle + \frac{\tilde{\gamma}}{2}[\langle\sigma_{i-1}\sigma_j\rangle + \langle\sigma_{i+1}\sigma_j\rangle + \langle\sigma_i\sigma_{j-1}\rangle + \langle\sigma_i\sigma_{j+1}\rangle] \\ & + \frac{\tilde{\gamma}}{2}[-\langle\sigma_i\sigma_{i-1}\sigma_j\rangle + \langle\sigma_i\sigma_{i+1}\sigma_j\rangle - \langle\sigma_i\sigma_j\sigma_{j-1}\rangle + \langle\sigma_i\sigma_j\sigma_{j+1}\rangle], \end{aligned} \quad (\text{IV.11})$$

with now  $\tilde{\gamma} = \tanh\beta\Delta$ . Note how these two are, again, neither closed nor linear since the dynamic equation for the expected value involves the correlation function, and the one for the correlation function involves the three body correlation function as well. The found dynamical equations Eq. (IV.10, IV.11), however, resemble more to the Ising chain's in equation Eq. (II.18) since it also contains the terms  $\langle\sigma_{i-1}\rangle$  and  $\langle\sigma_{i+1}\rangle$ . This did not happen for the CvD model, in which the only involved one was  $\langle\sigma_i\rangle$ .

### D. Closing the Equations

The dynamic equations when  $\varrho_{ij}$  depends on the state of the spin, as we have seen, are generally speaking not closed. This complicates things. Studying the steady state properties of any system by writing the dynamic equations, when they are not closed, leads nowhere.

However, if one writes down the obtained dynamical equations in Eq. (IV.3, IV.4) and Eq. (IV.6, IV.7) for

where  $\tilde{\gamma} = \tanh 2\beta\Delta$ . As we can see, these two, in contrast to the dynamic equations of the Ising chain, are not closed. The correlation function appears now in the differential equation for the expected value, and three body correlation functions appear in the differential equation for the two body one. This set is then, neither closed nor a linear system of differential equations.

### C. Vision Cone Model (VC)

The same thing can be done for the VC model. The nearest neighbour restriction of  $\varrho_{ij}$  can be done by imposing that a spin only looks to its right depending on its state, so that  $\varrho_{ij} = \delta_{(\sigma_i,-)}\delta_{i-1,j} + \delta_{(\sigma_i,+)}\delta_{i+1,j}$ . Now a spin  $\sigma_i$  pointing upwards will try to mimic spin  $\sigma_{i+1}$  while, if it points downwards it will try to mimic  $\sigma_{i-1}$  when  $\Delta > 0$ .

The VC model then includes a 0 on a side of the diagonal of  $\varrho_{ij}$  and a 1 on the opposite, and hence is of the second type (Appendix. D2) of definition of  $\varrho_{ij}$  discussed above. Taking into account that  $\delta_{(\sigma_i,\pm)} = (1 \pm \sigma_i)/2$ , the dynamic equations read

occupation state variables  $n_i = 0, 1$  instead of the Ising ones, by setting  $\sigma_i = 2n_i - 1$ , one can see how the obtained dynamical equations for the expected value  $\langle n_i \rangle$  and the correlation function  $\langle n_i n_j \rangle$  resemble a lot to the dynamical equations of the asymmetric exclusion process (ASEP) [17], which are also not closed (see Appendix E).

The fact that our dynamic equations resemble to the ones attributed to models like the ASEP model is telling us that it may be possible to analytically solve the steady state behaviour by using the matrix ansatz [17], which is a formal way of determining all the correlation functions at once, for the steady state. This similarity is also signaling the existence of steady currents, which represent a class of steady solutions of the ASEP model [17]. Note how this is strongly related to the existence of the traveling states observed in non-reciprocally interacting systems [8]. Before studying this possibility, however, one should also study if the dynamical equations we derived do find a steady state. One should note that the dynamical equations we derived were found by using spin flip dynamics, which does not conserve the order param-

eter, say the magnetization, while models like the ASEP model do conserve the order parameter, and belong to the universal class of model B [15].

Even if we derived, however, the equations using spin flip rates, the similarity between the ASEP model's dynamical equations and ours is also telling us that there may be conserved quantities in the models we covered. This is so because the dynamical equations of the ASEP model do conserve its order parameter.

Furthermore, with the aim of closing the dynamical equations, one could make some approximations. For instance, one could take the MF approximation by setting  $\langle \sigma_i \sigma_j \rangle = \langle \sigma_i \rangle \langle \sigma_j \rangle$ , such that now the dynamical equations for the expectation values in Eq. (IV.3, IV.6) are closed, even if still not linear. One could then linearize the system of equations and study the stability of fixed points, such as  $\langle \sigma_i \rangle = 0$  for any  $i = 1, \dots, N$ . The other possibility would be making the pair correlation approximation, which breaks correlations at three body terms.

## V. CONCLUSIONS

Following the results reviewed of the kinetic Ising model, in both the MF approximation and for  $d = 1$  Ising chains, we have presented a way of generalizing the Ising model in order to include the possibility of non-reciprocal interactions among spins. We have focused on investigating situations in which the non-reciprocal interactions appear due to the intrinsic state of each spin, which is a common situation in systems like fish banks, bird flocking, predator-prey dynamics and opinion formation.

The generalization of the Ising model has been done by taking as starting point the kinetic Ising model using Glauber dynamics, and, more specifically, the local field controlling the temperature dependent spin flip rates that govern the dynamics of the system of spins. Furthermore, we have presented two models, the CvD and VC models, in order to portray realistic situations in which non-reciprocal interactions display a relevant role, and were able to derive and characterize the MF stationary solutions analytically when considering that the asymmetric part of the interaction is way smaller than the global, symmetric one, by means of using perturbation theory. We have also studied the extension of this generalization to  $d = 1$  spin chains, and were able to find

the dynamical equations, in this case, for the CvD and VC models, and systematically compared the obtained results with the already known ones.

As we have seen, the stationary MF solutions of the CvD and VC models appear to share properties which do not appear in the usual, reciprocal, Ising model, such as the asymmetry of the positive and negative branches of the self consistent states, inducing the lack of  $\mathbb{Z}^2$  symmetry, as well as discontinuities in the magnetization, the non-uniqueness of the critical temperature and the metastability observed in both the simulations and the integrated free energy, strongly related to the loss of the  $\mathbb{Z}^2$  symmetry. We have seen how, all of the results, including the self consistent states, the critical temperature and the free energy reduce to the Ising model's MF ones taking the proper limit.

Additionally, we have seen how the dynamical equations for  $d = 1$  spin chains of the CvD and the VC model differ greatly from the dynamical equations for  $d = 1$  Ising chains, since they are now neither closed nor linear. The fact that the dynamical equations are not closed makes studying stationary states hard. We have seen, however, how the obtained dynamical equations resemble quite a lot the ones governing the dynamics in the asymmetric exclusion process. This signals the possibility of studying stationary states using the matrix ansatz, and the fact that a quantity may be conserved, even if the global magnetization of the system is not. These conserved quantities, again, may be strongly related to the existence of steady currents or traveling states.

In conclusion, our extension of the Ising model including non-reciprocal interactions, as well as the two proposed models, is able to give rise to new and diverse properties. Future work could be done in order to fully characterize the dynamical behaviour of non-reciprocal  $d = 1$  spin chains in order to understand how it differs from the dynamical behaviour of reciprocal Ising chains, as well as phase behaviour in finite dimensions.

## Acknowledgments

I would like to thank Demian Levis for his help and guidance, his valuable comments and suggestions throughout this work. I would also like to thank Ot Garcés, Kader Morkoç and my family for the unconditional support and interest.

- 
- [1] S. H. L. Klapp, *Nat. Nanotechnol.* **18**, 8–9 (2023).
  - [2] S. Osat and R. Golestanian, *Nature Nanotechnology* **18**, 79 (2023).
  - [3] J. Agudo-Canalejo and R. Golestanian, *Phys. Rev. Lett.* **123**, 018101 (2019).
  - [4] S. Saha, J. Agudo-Canalejo, and R. Golestanian, *Phys. Rev. X* **10**, 041009 (2020).
  - [5] A. Crisanti and H. Sompolinsky, *Phys. Rev. A* **37**, 4865 (1988).
  - [6] A. Crisanti and H. Sompolinsky, *Phys. Rev. A* **36**, 4922 (1987).
  - [7] V. Ros, F. Roy, G. Biroli, G. Bunin, and A. M. Turner, *Phys. Rev. Lett.* **130**, 257401 (2023).
  - [8] M. Fruchart, R. Hanai, P. B. Littlewood, and V. Vitelli, *Nature* **592**, 363–369 (2021).
  - [9] G. Xu, X. Zhou, Y. Li, Q. Cao, W. Chen, Y. Xiao,

- L. Yang, and C.-W. Qiu, *Phys. Rev. Lett.* **130**, 266303 (2023).
- [10] Z. You, A. Baskaran, and M. C. Marchetti, *Proceedings of the National Academy of Sciences* **117**, 19767 (2020).
- [11] D. S. Seara, A. Piya, and A. P. Tabatabai, *J. Stat. Mech.* **2023**, 043209 (2023).
- [12] R. J. Glauber, *J. Math. Phys.* **4**, 294 (1963).
- [13] N. van Kampen, *Stochastic Processes in Physics and Chemistry* (Elsevier Science Publishers, Amsterdam, 1992).
- [14] P. L. Krapivsky, S. Redner, and E. Ben-Naim, *A Kinetic View of Statistical Physics* (Cambridge University Press, 2010).
- [15] P. C. Hohenberg and B. I. Halperin, *Rev. Mod. Phys.* **49**, 435 (1977).
- [16] S. A. M. Loos, S. H. L. Klapp, and T. Martynec, *Phys. Rev. Lett.* **130**, 198301 (2023).
- [17] B. Derrida, *J. Stat. Mech.* **2007**, P07023 (2007).

## VI. APPENDIX

## Appendix A: One and Two Body Correlation Function Dynamic Equations

Consider an observable  $\mathcal{O}(\boldsymbol{\sigma})$ , with no implicit time dependence (it is a measure of the configuration of the spins). Then, we know that, by definition

$$\langle \mathcal{O} \rangle_t = \sum_{\{\boldsymbol{\sigma}\}} \mathcal{O}(\boldsymbol{\sigma}) p(\boldsymbol{\sigma}; t). \quad (\text{A.1})$$

If the rate of flipping spin  $\sigma_i$  is  $\omega_i(\sigma_i)$ , the master equation for spin flips writes,

$$\frac{d}{dt} p(\boldsymbol{\sigma}; t) = \sum_i [\omega(\sigma^i) p(\boldsymbol{\sigma}^i; t) - \omega(\sigma_i) p(\boldsymbol{\sigma}; t)], \quad (\text{A.2})$$

where if  $\boldsymbol{\sigma} = (\sigma_1, \dots, \sigma_i, \dots, \sigma_N)^T$ , then  $\boldsymbol{\sigma}^i = (\sigma_1, \dots, -\sigma_i, \dots, \sigma_N)^T$  after flipping spin  $\sigma_i$ . Using for notation (after the flip)  $\sigma^i = -\sigma_i$ . Now, we can change  $p(\boldsymbol{\sigma}; t)$  by  $\mathcal{O}(\boldsymbol{\sigma}) p(\boldsymbol{\sigma}; t)$ , so that, summing over all the configurations  $\{\boldsymbol{\sigma}\}$ ,

$$\begin{aligned} \sum_{\{\boldsymbol{\sigma}\}} \frac{d}{dt} [\mathcal{O}(\boldsymbol{\sigma}) p(\boldsymbol{\sigma}; t)] &=: \frac{d}{dt} \langle \mathcal{O} \rangle_t \\ &= \sum_{\{\boldsymbol{\sigma}\}} \sum_i [\omega(\sigma^i) \mathcal{O}(\boldsymbol{\sigma}) p(\boldsymbol{\sigma}^i; t) - \omega(\sigma_i) \mathcal{O}(\boldsymbol{\sigma}) p(\boldsymbol{\sigma}; t)]. \end{aligned} \quad (\text{A.3})$$

In order to perform the sum over all the configurations, we will separate this sums into two, so that

$$\frac{d\langle \mathcal{O} \rangle_t}{dt} = \sum_{\{\boldsymbol{\sigma}\}} \sum_i \mathcal{O}(\boldsymbol{\sigma}) \omega(\sigma^i) p(\boldsymbol{\sigma}^i; t) - \sum_{\{\boldsymbol{\sigma}\}} \sum_i \mathcal{O}(\boldsymbol{\sigma}) \omega(\sigma_i) p(\boldsymbol{\sigma}; t).$$

The term on the right is just the expected value of  $\mathcal{O}(\boldsymbol{\sigma}) \omega(\sigma_i)$ . The term on the left is a little harder. However, since we are summing over all the possible configurations, we can make the change of variables  $\boldsymbol{\sigma} \rightarrow \boldsymbol{\sigma}^i$ , so that  $\boldsymbol{\sigma}^i \rightarrow (\boldsymbol{\sigma}^i)^i = \boldsymbol{\sigma}_i$ , and, as a consequence,

$$\begin{aligned} \frac{d\langle \mathcal{O} \rangle_t}{dt} &= \sum_{\{\boldsymbol{\sigma}^i\}} \sum_i \mathcal{O}(\boldsymbol{\sigma}^i) \omega((\boldsymbol{\sigma}^i)^i) p((\boldsymbol{\sigma}^i)^i; t) - \sum_{\{\boldsymbol{\sigma}\}} \sum_i \mathcal{O}(\boldsymbol{\sigma}) \omega(\sigma_i) p(\boldsymbol{\sigma}; t) \\ &= \sum_i \sum_{\{\boldsymbol{\sigma}^i\}} \mathcal{O}(\boldsymbol{\sigma}^i) \omega(\sigma_i) p(\boldsymbol{\sigma}; t) - \sum_i \sum_{\{\boldsymbol{\sigma}\}} \mathcal{O}(\boldsymbol{\sigma}) \omega(\sigma_i) p(\boldsymbol{\sigma}; t) \\ &= \sum_i \langle \mathcal{O}(\boldsymbol{\sigma}^i) \omega(\sigma_i) \rangle_t - \sum_i \langle \mathcal{O}(\boldsymbol{\sigma}) \omega(\sigma_i) \rangle_t = \boxed{\sum_i \langle [\mathcal{O}(\boldsymbol{\sigma}^i) - \mathcal{O}(\boldsymbol{\sigma})] \omega(\sigma_i) \rangle_t}. \end{aligned} \quad (\text{A.4})$$

If we now set  $\mathcal{O}(\boldsymbol{\sigma}) = \sigma_k$  or  $\mathcal{O}(\boldsymbol{\sigma}) = \sigma_k \sigma_\ell$ , we can easily find the time evolution of the average spin and the correlation function.

- (i) For instance, by taking  $\mathcal{O}(\boldsymbol{\sigma}) = \sigma_k$ , we will have that  $d\langle \mathcal{O} \rangle_t / dt = d\langle \sigma_k \rangle_t / dt$ . Besides, since  $\sigma^i := -\sigma_i$ ,  $\mathcal{O}(\boldsymbol{\sigma}^i) - \mathcal{O}(\boldsymbol{\sigma}) = (\sigma^k - \sigma_k) \delta_{ik} =: -2\sigma_k \delta_{ik}$ , as the difference  $\sigma_k(\boldsymbol{\sigma}^i) - \sigma_k(\boldsymbol{\sigma})$  will only be different than zero if the spin flipped is spin  $k$  (note how we sum over every single flip of spin  $i$ ). Thus, now equation Eq. (A.4) reads,

$$\frac{d\langle \sigma_k \rangle_t}{dt} = \sum_i \langle (-2\sigma_k) \delta_{ik} \omega(\sigma_i) \rangle_t = -2\langle \sigma_k \omega(\sigma_k) \rangle_t. \quad (\text{A.5})$$

- (ii) Samewise, by taking  $\mathcal{O} = \sigma_k \sigma_\ell$ , we will have,  $\mathcal{O}(\boldsymbol{\sigma}^i) - \mathcal{O}(\boldsymbol{\sigma}_i) = -2\sigma_k \sigma_\ell (\delta_{ik} + \delta_{i\ell})$  since now the difference  $\mathcal{O}(\boldsymbol{\sigma}^i) - \mathcal{O}(\boldsymbol{\sigma})$  will only be different than zero if either  $i = k$  or  $i = \ell$ . As a consequence, we will have,

$$\frac{d\langle \sigma_k \sigma_\ell \rangle_t}{dt} = \sum_i \langle -2\sigma_k \sigma_\ell (\delta_{ik} + \delta_{i\ell}) \omega(\sigma_i) \rangle_t = -2\langle \sigma_k \sigma_\ell [\omega(\sigma_k) + \omega(\sigma_\ell)] \rangle_t. \quad (\text{A.6})$$

Appendix B: Mean Field Dynamic Equation for the Vision Cone Model,  $|\Delta| \ll J$ 

Using the definition for the Vision Cone (VC) model,  $\varrho_{ij} = \delta_{(\sigma_i, -)}\Theta(j < i) + \delta_{(\sigma_i, +)}\Theta(j > i)$  the dynamical equation for  $m$  can be computed. First note how since  $\sigma_i$  is an Ising variable, the Kronecker deltas in the definitions can be written as,

$$\delta_{(\sigma_i, -)} = \frac{1 - \sigma_i}{2}, \quad \delta_{(\sigma_i, +)} = \frac{1 + \sigma_i}{2}. \quad (\text{B.1})$$

We will then have that,

$$\begin{aligned} \langle \sigma_i \delta \omega_i \rangle &= -\frac{\beta}{2} \operatorname{sech}^2 \beta N J m \sum_j \langle \varrho_{ij} \sigma_j \rangle \\ &= -\frac{\beta}{2} \operatorname{sech}^2(\beta N J m) \sum_j \langle [\delta_{(\sigma_i, -)}\Theta(j < i) + \delta_{(\sigma_i, +)}\Theta(j > i)] \sigma_j \rangle \\ &= -\frac{\beta}{4} \operatorname{sech}^2(\beta J N m) \left[ \sum_{j < i} \left\langle \left( \frac{1 - \sigma_i}{2} \right) \sigma_j \right\rangle + \sum_{j > i} \left\langle \left( \frac{1 - \sigma_i}{2} \right) \sigma_j \right\rangle \right] \end{aligned} \quad (\text{B.2})$$

We can now take the MF approximation  $\langle \sigma_i \sigma_j \rangle = \langle \sigma_i \rangle \langle \sigma_j \rangle$  for  $j \neq i$ . By doing so, one obtains,

$$\langle \sigma_i \delta \omega_i \rangle = -\frac{\beta}{2} \operatorname{sech}^2(\beta N J m) \left[ \sum_{j \neq i} \langle \sigma_j \rangle + \langle \sigma_i \rangle \left( \sum_{j > i} \langle \sigma_j \rangle - \sum_{j < i} \langle \sigma_j \rangle \right) \right]. \quad (\text{B.3})$$

The first sum of the latter can be directly approximated by  $Nm$ . The two other sums, however, are not as trivial. As expected, spin  $i$  divide a chain of spins into two, and so it appears to be the upper and lower bound of both. In order to perform this summations, we have to take the thermodynamic limit when  $J := 1/N$  and  $N \rightarrow \infty$ , such that if we imagine the two halves to be identical, since they are both infinitely long, both summation will converge to the same object, and we will be able to, in this case, identify every spin of both chains (separated by  $i$ ) as identical, and of magnitude  $m = \langle \sigma_j \rangle$  for all  $j \neq i$ . We will make the assumption that if  $N$  is big enough, this approximation still holds, and then take the thermodynamic limit. In this situation, then

$$\begin{aligned} \langle \sigma_i \delta \omega_i \rangle &\approx -\frac{\beta}{2} \operatorname{sech}^2(\beta N J m) \left[ Nm + \langle \sigma_i \rangle \left( \sum_{j > i} m - \sum_{j < i} m \right) \right] \\ &= -\frac{\beta}{4} \operatorname{sech}^2(\beta N J m) [Nm + \langle \sigma_i \rangle m (N - (i + 1) - (i - 1))] \\ &= -\frac{\beta N m}{4} \left[ 1 + \langle \sigma_i \rangle \left( 1 - 2 \frac{i}{N} \right) \right] \operatorname{sech}^2(\beta N j m). \end{aligned} \quad (\text{B.4})$$

In here  $i/N$  is the relative position of spin  $\sigma_i$  on the chain. However, when making the MF approximation, the sense of chain and lattice doesn't apply anymore. Taking into account that  $i/N$  also represents the fraction of spins that are being overlooked by  $\sigma_i$  when considering a fully connected model (since its relative position is  $i/N$ ), we will define  $z := i/N$  the fraction of overlooked neighbors as a MF parameter, so that when we take the thermodynamic limit and lose sense of geometry, we still have a well defined way of understanding the geometrical influence of having a vision field. By doing so, again, we will have, then

$$\langle \sigma_i \delta \omega_i \rangle = -\frac{\beta N m}{4} [1 + \langle \sigma_i \rangle (1 - 2z)] \operatorname{sech}^2(\beta N J m). \quad (\text{B.5})$$

We can hence add this one to the contribution of the symmetric (reciprocal) field in order to get the dynamic equation for  $\langle \sigma_i \rangle$  as portrayed in equation Eq. (II.18), then divide by  $N$  and sum over all spins to find the dynamic equation of  $m$ .

Appendix C: Generalized Mean Field Dynamic Equation,  $|\Delta| \ll J$ 

The dynamical equations found for both the CvD and VC models in the  $|\Delta| \ll J$  limit can be generally written when  $\varrho_{ij} = \psi(\sigma_i)(1 - \delta_{ij})$ . We have seen how in the  $|\Delta| \ll J$  limit the rates take the shape  $\omega(\sigma_i, \Delta) = \omega^0(\sigma_i) + \Delta\delta\omega_i + \mathcal{O}(\Delta^2)$ , and then the dynamical equation for  $\langle\sigma_i\rangle$ , Eq. (II.8), becomes

$$\frac{d\langle\sigma_i\rangle}{dt} = -2\langle\sigma_i\omega(\sigma_i, \Delta)\rangle = -2\langle\sigma_i\omega^0(\sigma_i)\rangle - 2\Delta\langle\sigma_i\delta\omega_i\rangle + \mathcal{O}(\Delta^2), \quad (\text{C.1})$$

where  $\omega^0(\sigma_i) = \frac{1}{2}[1 - \sigma_i \tanh(\beta h_s^i)]$  and

$$\delta\omega_i = -\frac{\beta}{2} \text{sech}^2 \beta h_s^i \sigma_i \sum_{j=1}^N \varrho_{ij} \sigma_j, \quad h_s^i = \sum_{j=1}^N J_{ij}^s \sigma_j.$$

Plugging the latter two into equation Eq. (C.1) and using that  $\sigma_i^2 = 1$  for any  $i$ ,

$$\frac{d\langle\sigma_i\rangle}{dt} = -\langle\sigma_i\rangle + \langle\tanh \beta h_s^i\rangle + \beta\Delta \left\langle \text{sech}^2 \beta h_s^i \sum_{j=1}^N \varrho_{ij} \sigma_j \right\rangle, \quad (\text{C.2})$$

such that, taking the MF approximation for the symmetric part of the field  $h_s^i$  considering the usual definition of the FC Ising model  $J_{ij}^s = J(1 - \delta_{ij})$ ,  $J = 1/N$ , we had  $h_s^i \approx NJm$ , and, finally,

$$\frac{d\langle\sigma_i\rangle}{dt} = -\langle\sigma_i\rangle + \tanh(\beta NJm) + \beta\Delta \text{sech}^2(\beta NJm) \sum_{j=1}^N \langle\varrho_{ij} \sigma_j\rangle. \quad (\text{C.3})$$

We can now plug  $\varrho_{ij} = \psi(\sigma_i)(1 - \delta_{ij})$ , divide both sides by  $N$  and sum over all  $i$  to find

$$\begin{aligned} \frac{1}{N} \sum_{i=1}^N \frac{d\langle\sigma_i\rangle}{dt} &= -\frac{1}{N} \sum_{i=1}^N \langle\sigma_i\rangle + \frac{1}{N} \sum_{i=1}^N \tanh(\beta NJm) + \beta\Delta \text{sech}^2(\beta NJm) \frac{1}{N} \sum_{i=1}^N \sum_{j=1}^N \langle\psi(\sigma_i)\sigma_j(1 - \delta_{ij})\rangle \iff \\ \frac{dm}{dt} &= -m + \tanh(\beta NJm) + \beta\Delta \text{sech}^2(\beta NJm) \frac{1}{N} \sum_{i=1}^N \sum_{j \neq i}^N \langle\psi(\sigma_i)\rangle \langle\sigma_j\rangle \iff . \end{aligned} \quad (\text{C.4})$$

By defining  $K = \beta NJ$  the last one can be written,

$$\frac{dm}{dt} = -m + \tanh Km + \beta\Delta \text{sech}^2 Km \frac{1}{N} \sum_{i=1}^N \sum_{j \neq i}^N \langle\psi(\sigma_i)\rangle \langle\sigma_j\rangle. \quad (\text{C.5})$$

The tricky part of the last one can be finding a way of defining  $\psi(\sigma_i)$  which makes it possible to express the third term on the right hand side of the equation expressed as a function of the magnetization. If one does so, then one should be able to write

$$\frac{dm}{dt} = \varphi_0(m; K) + \Delta\tilde{\varphi}(m; K, \epsilon), \quad \varphi_0(m; K) = -m + \tanh Km, \quad (\text{C.6})$$

where  $\epsilon$  represents possible parameters that appear due to the definition of  $\psi(\sigma_i)$ . Note how  $\varphi_0(m; K) = -\varphi_0(-m; K)$ , while  $\varphi(m; K, \epsilon)$  is not subject to any symmetry in general. This is why we see a violation of the  $\mathbb{Z}^2$  symmetry and why all the results for  $\Delta = 0$  ( $q = 0$ ) returns the MF results. Note how the free energy of any definition of  $\psi(\sigma_i)$  that allows for a description of the magnetization of the shape in Eq. (C.6) is just

$$\mathcal{F}(m; K, \Delta, \epsilon) = \mathcal{F}_0(K) - \int \varphi_0(m; K) dm - \Delta \int \tilde{\varphi}(m; K, \epsilon) dm. \quad (\text{C.7})$$

Note how in the case of the CvD and VC models we defined  $\varphi(m; K, q, \epsilon) = q\tilde{\varphi}(m; K, \epsilon)$ , such that  $q = \Delta/J$ .

**Appendix D: Constraints (I) & (II) on  $\varrho_{ij}$** 
**1. Constraint (I)**

Let's show that the condition imposed for the first  $\Delta$  dynamics,

$$\frac{1}{2} \sum_{j \in \langle i \rangle} \varrho_{ij} \sigma_j = 0, \pm 1, \quad (\text{D.1})$$

holds when  $\varrho_{ij} = \pm 1$  for all  $j \in \langle i \rangle$ . In to do so, we only need to use the fact that  $\sigma_j$  are Ising variables, so that the following table follows straight ahead,

$\sigma_{i-1}$	$\sigma_{i+1}$	$\frac{1}{2} \sum_{j \in \langle i \rangle} \varrho_{ij} \sigma_j$
+1	+1	$\frac{1}{2}(\varrho_{i,i-1} + \varrho_{i,i+1})$
+1	-1	$\frac{1}{2}(\varrho_{i,i-1} - \varrho_{i,i+1})$
-1	+1	$\frac{1}{2}(-\varrho_{i,i-1} + \varrho_{i,i+1})$
-1	-1	$\frac{1}{2}(-\varrho_{i,i-1} - \varrho_{i,i+1})$

TABLE I: Table showing all the possible values of the term that appears on the rate, to justify the condition appearing after the condition in equation Eq. (D.1).

All of these sum compute to  $0, \pm 1$  if we consider  $\varrho_{ij}$  also to be Ising like variables.

**2. Constraint (II)**

Let's now verify that the type II definition of  $\varrho_{ij}$ , for which  $\varrho_{ij}$  is composed of a zero on one side of the diagonal and a  $\pm 1$  on the other one, verifies the imposed condition,

$$\sum_{j \in \langle i \rangle} \varrho_{ij} \sigma_i = 0, \pm 1. \quad (\text{D.2})$$

We can do so looking a the following simple table.

$\varrho_{i,i-1}$	$\varrho_{i,i+1}$	$\sum_{j \in \langle i \rangle} \varrho_{ij} \sigma_j$
0	$\pm 1$	$\pm \sigma_{i+1}$
$\pm 1$	0	$\pm \sigma_{i-1}$

TABLE II: Possible values regarding the local field for the strict Vision Cone model.

Again, since  $\sigma_i$  are Ising variables, the possible results are always  $\pm 1$ , and so they verify the imposed condition in equation Eq. (D.2).

**Appendix E: Occupation State Dynamic Equations**

The dynamic equations for a  $d = 1$  chain when  $J_{ij}^s = 0$ , such that  $J_{ij} = \Delta \varrho_{ij}$ , for the cases discussed in section Sec. IV write

$$\frac{d\langle \sigma_i \rangle}{dt} = -\langle \sigma_i \rangle + \gamma \sum_{k \in \langle i \rangle} \langle \varrho_{ik} \sigma_k \rangle \quad (\text{E.1})$$

$$\frac{d\langle \sigma_i \sigma_j \rangle}{dt} = -2\langle \sigma_i \sigma_j \rangle + \gamma \left\langle \sigma_j \sum_{k \in \langle i \rangle} \varrho_{ik} \sigma_k \right\rangle + \gamma \left\langle \sigma_i \sum_{\ell \in \langle j \rangle} \varrho_{j\ell} \sigma_\ell \right\rangle, \quad (\text{E.2})$$

where  $\gamma = \frac{1}{2} \tanh 2\beta\Delta$ ,  $\tanh \beta\Delta$  depending if  $\varrho_{ij}$  was a type I (D 1) matrix or a type II (D 2) one. Deriving the dynamic equations for the expectation value and the correlation function, now for occupation states instead of Ising variables,

can be done by plugging  $\sigma_i = 2n_i - 1$  into the dynamical equations above. Not however, that these dynamical equations have been derived from a spin flip dynamical point of view. We will have,  $d\langle\sigma_i\rangle/dt = d\langle 2n_i - 1\rangle/dt = 2d\langle n_i\rangle/dt$ , and samewise,  $\langle\sigma_i\rangle = 2\langle n_i\rangle - 1$ . Furthermore, since  $\varrho_{ik}\sigma_k = \varrho_{ik}(2n_k - 1) = 2\varrho_{ik}n_k - \varrho_{ik}$ , we will have, following equations Eq. (E.1, E.2)

$$\frac{d\langle n_i\rangle}{dt} = \frac{1}{2} \left( 1 - \gamma \sum_{k \in \langle i \rangle} \langle \varrho_{ik} \rangle \right) - \langle n_i \rangle + \gamma \left\langle \sum_{k \in \langle i \rangle} \varrho_{ik} n_k \right\rangle. \quad (\text{E.3})$$

The same thing can be done to obtain the correlation function's dynamical equation. Now we will have that,  $\langle\sigma_i\sigma_j\rangle = \langle(2n_i - 1)(2n_j - 1)\rangle$ , so that, developing the products,  $\langle\sigma_i\sigma_j\rangle = 4\langle n_i n_j \rangle - 2\langle n_i \rangle - 2\langle n_j \rangle + 1$ . Since now  $d\langle\sigma_i\sigma_j\rangle/dt = 4d\langle n_i n_j \rangle/dt - 2d\langle n_i \rangle/dt - 2d\langle n_j \rangle/dt$ , we can combine equations Eq. (E.3) and Eq. (E.1) to find, after some trivial algebraic manipulation,

$$\begin{aligned} \frac{d\langle n_i n_j \rangle}{dt} &= \frac{1}{2} [\langle n_i \rangle + \langle n_j \rangle] - 2\langle n_i n_j \rangle \\ &+ \frac{\gamma}{2} \left\langle n_j \sum_{k \in \langle i \rangle} \varrho_{ik} (2n_k - 1) \right\rangle + \frac{\gamma}{2} \left\langle n_i \sum_{\ell \in \langle j \rangle} \varrho_{j\ell} (2n_\ell - 1) \right\rangle. \end{aligned} \quad (\text{E.4})$$

By means of plugging the definition of either the CvD or the VC model one can see how, again, these equations are not closed either.